

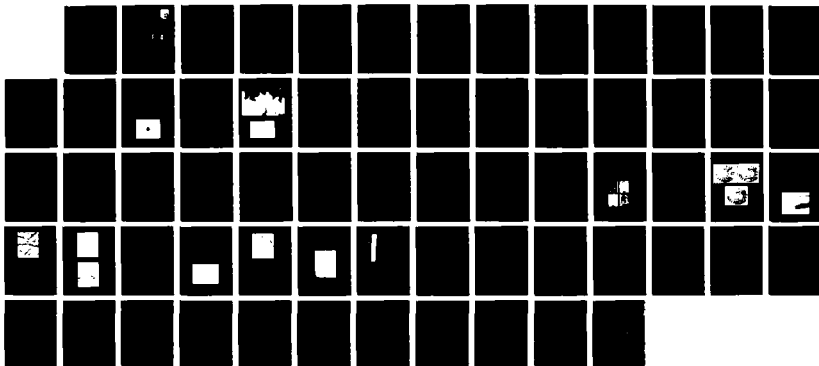
AD-A104 961

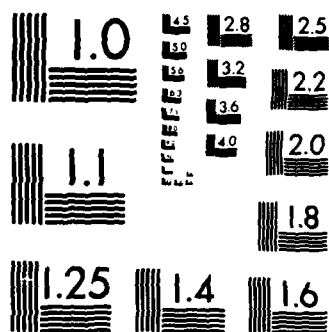
CHARACTERIZATION OF THE MICROSTRUCTURES OF VARIOUS  
MATERIALS(U) SYSTEMS RESEARCH LABS INC DAYTON OH  
RESEARCH APPLICATIONS DIV A G JACKSON JUN 87 SRL-6010

1/1

UNCLASSIFIED AFMRL-TR-87-4041 F33615-83-C-5073

F/G 11/6.1 NL

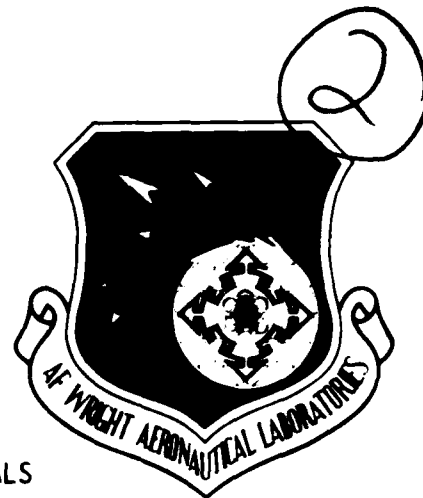




MICROCOPY RESOLUTION TEST CHART  
NATIONAL BUREAU OF STANDARDS-1963-A

**AD-A184 961**

AFWAL-TR-87-4041



CHARACTERIZATION OF THE MICROSTRUCTURES OF VARIOUS MATERIALS

Allen G. Jackson, Ph.D.

Research Applications Division  
Systems Research Laboratories, Inc.  
2800 Indian Ripple Road  
Dayton, OH 45440-3696

DTIC  
ELECTE  
SEP 16 1987  
S D  
C&D

June 1987

Final Report for Period 1 September 1983 - 31 August 1986

Approved for public release; distribution is unlimited.

MATERIALS LABORATORY  
AIR FORCE WRIGHT AERONAUTICAL LABORATORIES  
AIR FORCE SYSTEMS COMMAND  
WRIGHT-PATTERSON AIR FORCE BASE, OH 45433-6533

UNCLASSIFIED

SECURITY CLASSIFICATION OF THIS PAGE

## REPORT DOCUMENTATION PAGE

1a. REPORT SECURITY CLASSIFICATION <b>Unclassified</b>			1b. RESTRICTIVE MARKINGS		
2a. SECURITY CLASSIFICATION AUTHORITY			3. DISTRIBUTION/AVAILABILITY OF REPORT Approved for public release; distribution is unlimited.		
2b. DECLASSIFICATION/DOWNGRADING SCHEDULE					
4. PERFORMING ORGANIZATION REPORT NUMBER(S)  6810 Final			5. MONITORING ORGANIZATION REPORT NUMBER(S)  AFWAL-TR-87-4041		
6a. NAME OF PERFORMING ORGANIZATION Systems Research Laboratories, Inc.		6b. OFFICE SYMBOL (If applicable)	7a. NAME OF MONITORING ORGANIZATION Air Force Wright Aeronautical Laboratories Materials Laboratory (AFWAL/MLLS)		
6c. ADDRESS (City, State and ZIP Code) 2800 Indian Ripple Rd. Dayton, OH 45440-3696			7b. ADDRESS (City, State and ZIP Code) Wright Patterson AFB, OH 45433-6533		
8a. NAME OF FUNDING/SPONSORING ORGANIZATION		8b. OFFICE SYMBOL (If applicable)	9. PROCUREMENT INSTRUMENT IDENTIFICATION NUMBER F33615-83-C-5073		
8c. ADDRESS (City, State and ZIP Code)			10. SOURCE OF FUNDING NOS.		
			PROGRAM ELEMENT NO.	PROJECT NO.	TASK NO.
			62102F	2418	01
11. TITLE (Include Security Classification) CHARACTERIZATION OF THE MICROSTRUCTURES OF VARIOUS MATERIALS			WORK UNIT NO. 31		
12. PERSONAL AUTHOR(S) Allen G. Jackson					
13a. TYPE OF REPORT Final		13b. TIME COVERED FROM 83-9-1 TO 86-8-31		14. DATE OF REPORT (Yr., Mo., Day) June 1987	
15. PAGE COUNT 65					
16. SUPPLEMENTARY NOTATION					
17. COSATI CODES			18. SUBJECT TERMS (Continue on reverse if necessary and identify by block number)		
FIELD	GROUP	SUB. GR.			
11	06		Charcterization Ti Alloys Al Alloys		
14	02		Electron Microscopy Rapid Solidification		
			Metallography Analytical Electron Microscopy		
19. ABSTRACT (Continue on reverse if necessary and identify by block number) Characterization research was conducted on Ti-, Al-, and Mg-base alloys and nonmetallic polymers using electron-optical and light optical methods, including transmission, scanning transmission and scanning electron microscopy, electron microprobe, interference layer microscopy, and various light optical methods. Rapid solidification research was done on Ti-, Al-, and Mg-base alloys using pendant-drop-melt-extraction, melt-spinning, and splat cooling methods. Apparatus to produce the alloys was constructed.					
20. DISTRIBUTION/AVAILABILITY OF ABSTRACT UNCLASSIFIED/UNLIMITED <input checked="" type="checkbox"/> SAME AS RPT. <input type="checkbox"/> DTIC USERS <input type="checkbox"/>			21. ABSTRACT SECURITY CLASSIFICATION Unclassified		
22a. NAME OF RESPONSIBLE INDIVIDUAL Charles R. Underwood			22b. TELEPHONE NUMBER (Include Area Code) (513) 255-4249		22c. OFFICE SYMBOL AFWAL/MLLS

DD FORM 1473, 83 APR

EDITION OF 1 JAN 73 IS OBSOLETE.

UNCLASSIFIED

SECURITY CLASSIFICATION OF THIS PAGE

## Preface

This report was prepared by A. G. Jackson, Ph.D., and covers work performed during the period 1 September 1983 through 31 August 1986 under Air Force Contract F33615-83-C-5073. Persons contributing to this effort were R. J. Bacon, R. D. Brodecki, F. O. Deutscher, C. E. Harper, J. C. Heidenreich, J. S. Hennessee, R. K. Lewis, P. F. Lloyd, A. S. Longo, R. E. Omlor, J. G. Paine, J. S. Paine, M. S. Rowe, and V. L. Weddington. The contract was administered under the direction of the Air Force Wright Aeronautical Laboratories, Materials Laboratory (AFWAL/MLLS), Wright-Patterson Air Force Base, OH, with Mr. Charles R. Underwood as Government Project Monitor.



Accession For	
NTIS CRA&I	<input checked="" type="checkbox"/>
DTIC TAB	<input type="checkbox"/>
Unannounced	<input type="checkbox"/>
Justification	
By	
Distribution /	
Availability Codes	
Dist	Avail and/or Special
A-1	

## TABLE OF CONTENTS

SECTION	PAGE
1 INTRODUCTION	1
BACKGROUND ON MATERIALS OF INTEREST	2
2 SUMMARY OF WORK PERFORMED	5
ELECTRON OPTICS	5
TEM/STEM	6
SEM	6
EPMA	6
AEM	6
Analysis of Al-Ho Alloy	7
Literature Review of Ti-6Al-4V	16
Ti6-Al-4V Phase Diagram	20
METALLOGRAPHY	28
Procedure for Polishing Ends of 3/4 x 3 x 7-in. Plexiglas Fatigue Specimens	31
Electrolytic Polishing Techniques for RST Ti Alloy Ribbons	33
Electropolishing vs Mechanical Polishing	38
SRL/R.A.R.E. SYSTEM	40
Results Obtained Using SRL/R.A.R.E. System	44
Summary	45
RAPID SOLIDIFICATION EQUIPMENT	47
3 PAPERS, PRESENTATIONS, EXHIBITS, AND INVENTIONS	49
PAPERS AND PRESENTATIONS	49
EXHIBITS	54
INVENTIONS	57

## LIST OF FIGURES

Figure	Page
1     Diffraction Pattern from Al-Ho.	8
2     (a) Bright Field of Grains in Al-Ho. (b) Diffraction Pattern from Area in 2(a).	10
3     Ti-6Al-4V Pseudo-Binary Phase Diagram.	21
4     Ti-V Binary Diagram Extrapolated from Ternary Data of Farrar and Margolin. <sup>13</sup>	22
5     Volume Fraction of $\beta$ as Function of Temperature (from Fopiano, Bever, and Averbach <sup>6</sup> ).	23
6     Plot of Maximum Lathe Size vs. Particle Size for Ti-6Al-4V Powder. <sup>18</sup>	24
7     Distance Diffused for V in Ti for Various Temperatures and Times.	24
8     IMI 829 Etched with New Procedure HT-A (F) or Part of Fin, HT-A (S) or Part of Shaft. HT-B (F) and HT-B (S) are same alloy but heat treated at higher temperature.	30
9     (a) Plexiglas under Low Load, (b) Medium Load, and (c) High Load.	32
10    Scanning Electron Micrograph of Electropolished Ti-9Co Showing Improved Detail of Grain Boundaries and Edge Retention at 400x.	33
11    Scanning Electron Micrograph of Electropolished Ti-9Co Showing Greatly Improved Definition of Coarse- $\alpha$ Precipi- tation from Grain Boundaries in Matrix of Fine $\alpha$ .	34

## LIST OF FIGURES (Concluded)

Figure		Page
12	Scanning Electron Micrograph of Mechanically Polished Ti-9Co Surface at 200x; Entire Surface is Rounded, Pitted.	35
13	Scanning Electron Micrograph of Mechanically Polished Ti-9Co; High-Magnification Resolution of Basket-Weave $\alpha$ .	35
14	Current-Voltage Curve for K-18 Series Ti-9Co (3 Min., 9-mm Developed at Diameter, $-30^{\circ}\text{C}$ ).	36
15	Current-Voltage Curve for K-18 Series Ti-9Co (60 Min. at $-45^{\circ}\text{C}$ ).	37
16	Energy-Dispersive Spectrum of Ti-4W.	37
17	Scanning Electron Micrograph of Ti-4W Rod Spark Eroded in Liquid Nitrogen. (2000x)	38
18	Mechanically Polished Ti-16Al-4V Rod after 50-gm Knoop Hardness Testing (133x).	39
19	Electropolished Ti-6Al-4V Rod after 50-gm Knoop Hardness Testing (133x).	40
20	Graph Showing Current vs Voltage Relationship for Ti-6Al-2Sn-4Zr-6Mo Specimen.	45
21	Graph Depicting Results Obtained for Electrolyte Temperature of $-60^{\circ}\text{C}$ for Ti-6Al-2Sn-4Zr-6Mo Specimen.	46
22	Graph Illustrating Effect of Varying Electrolyte Temperature $5^{\circ}\text{C}$ by Plotting both Sets of Data on Same Graph.	46



## LIST OF TABLES

<u>Table</u>	<u>Page</u>
1 Documented Compounds of Al-Ho	8
2 Planes and Interplanar Separations for $Al_2O_3$ (Lattice Constants are 3.1, 0, 4.99)	11
3 Planes and Interplanar Separations for $HoAl_3$ (Lattice Constants are 6.05, 0, 35.82)	12
4 Planes and Interplanar Separations for $HoAl_2$ (Lattice Constants are 7.814, 0, 0)	13
5 Planes and Interplanar Separations for $HoAl$ (Lattice Constants are 5.801, 11.34, 5.621)	13
6 Comparison of Measured and Calculated Distances in Several Compounds	15
7 Analysis of Al Matrix Diffraction Pattern	15
8 Analysis of Precipitate Diffraction Pattern	16
9 Microstructures Observed in Ti-6Al-4V for Various Types of Quench	18
10 Summary of Met Lab Statistics	29
11 Summary of Photo Lab Statistics	30
12 Comparison of Tests Performed on Mechanically Polished, Electropolished Specimens.	41

## SECTION 1

### INTRODUCTION

This report contains summaries of research performed under Contract F33615-83-C-5073 for the period 1 September 1983 through 31 August 1986. The research was performed in the Materials Characterization Facility at the AFWAL Materials Laboratory in accordance with the statement of work in the contract.

Characterization of the microstructures of new materials being developed by the Materials Laboratory is an essential step in assessing the value of such materials for Air Force applications. Materials characterized included both metals and nonmetals such as organic polymers, ceramics, and various types of composites. In accomplishing such characterization the techniques employed were electron-optical and light-optical microscopy encompassing qualitative and quantitative analyses of features, structures, and phases observed.

The overall objective of this research program, therefore, was to characterize the microstructures of new and improved materials being developed for use in aerospace-systems applications and to establish the conditions necessary to allow retention of these microstructures and associated properties in service use. The specific objective of the program was to characterize the microstructures of materials from AFWAL Materials Laboratory in-house investigations to obtain information concerning microstructural parameters associated with improvements in structural strength and stability. To reach this objective, exploratory research was conducted using characterization methods involving electron- and light-optical microscopy.

Within this program, characterization was defined as research to determine the morphology, composition, and crystallography of the materials of interest. Light-optical methods were employed on materials to obtain data to the micron level, while electron-optical methods were used for micron and submicron levels. Specific techniques employed were optical microscopy, quantitative microscopy, transmission electron microscopy (TEM), scanning transmission electron microscopy (STEM), analytical

electron microscopy (AEM), scanning electron microscopy (SEM), electron microprobe analysis (EPMA), energy- and wavelength-dispersive spectroscopy, energy-loss spectroscopy, and electron diffraction (selected area and convergent beam). Supplemental methods employed included differential scanning calorimetry, differential thermal analysis, X-ray diffraction, application of various computer models for structure analyses, and rapid solidification methods such as melt spinning, pendant drop melt extraction, and hammer/anvil splatting.

Materials of interest to the characterization research efforts were Ti alloys ( $\alpha$ ,  $\alpha + \beta$ , and  $\beta$  types), Al alloys, Mg alloys, and superalloys (Ni based), polymers, carbon-carbon composites, steels, metal-matrix composites, ceramics, and high-temperature alloys (Fe-, Ni-, refractory-metal based).

#### BACKGROUND ON MATERIALS OF INTEREST

Research on high-strength aluminum alloys encompassed most of the compositions that can be made using standard melting, ingot casting, and work processes. There is considerable evidence that emerging powder technology will lead to alloys having improved combinations of strength, toughness, and stress-corrosion resistance as compared to current alloys and perhaps even improved fatigue properties. Associated with these new alloys, however, is a class of microstructures not experienced in conventional alloys, and their role in controlling properties has not been established.

One of the aims of the research in the AFWAL Materials Laboratory is to examine microstructure/property relationships in order to anticipate possible problems with the aluminum-powder-technology area. This involves examining the role of the various microstructural features peculiar to powder alloys in the light of their effects upon the critical reliability properties of fatigue-crack-growth rate, toughness, and stress-corrosion resistance.

Continuing efforts to improve titanium alloys with respect to their performance, reliability, cost, and producibility seek to determine the

influence of metallurgical variables upon properties in order that processing and composition may be properly manipulated in such a way as to obtain the desired properties most effectively. The Materials Laboratory effort involves utilizing relationships between properties and microstructure of titanium alloys to develop those processes, heat treatments, and minor alloying changes which reduce scatter in measured properties as well as improve mean values. The activity centers around fatigue and creep properties but, by necessity, includes other properties for base-line data.

It is not currently possible to predict the mechanical properties of a material from its microstructure in a quantitative fashion. The ability to do so, however, would substantially reduce the amount of mechanical testing required to evaluate a material. Recognizing the increase in reliability and the cost savings that would result from the use of quantitative techniques, the Materials Laboratory has been active in the quantitative-metallography area in the past. The theme of the work has been the development of the techniques necessary for the recording of microstructural information in a form suitable for a computer and the development of the means for subsequently relating the microstructural information to the mechanical properties.

The quantitative-metallography effort has been concentrated mainly on titanium alloys since it is considered to be the most challenging area to pursue and the one where the need for quantitative techniques is greatest. However, the quantitative program was one of technique development and was directly related to the effort in microstructure/property relationships pursued in other areas of this program.

The utilization of ceramics in turbine engines offers significant potential for increased efficiency and lower cost. The Materials Laboratory activity covers the area of microstructural characterization and that area of mechanical behavior which is critical to the application of ceramics to turbines.

Increased emphasis has been placed by the Air Force on the durability of engines and airframes because of rapidly increasing acquisition and O & M

costs of advanced systems and the burden to the Air Force in maintaining fleet effectiveness at reasonable costs. One of the most significant results of the recognition of these problems was the introduction of the Damage Tolerant Design approach to new USAF airframes. Higher performance of advanced engines has produced a need to resort to more finite life components in engines. These problems have led to Materials Laboratory programs for development of improved techniques for predicting the service life of engine and airframe components and to investigations of means to mitigate the corrosion, stress-corrosion, and corrosion-fatigue behavior of aircraft structural materials.

The program on microstructural characterization complemented work in the above areas being carried out within the AFWAL Materials Laboratory. Unique equipment and specialized investigative techniques peculiar to this laboratory were used. The program provided the flexibility and versatility required for effective accomplishment of objectives in cooperation with the inherently diverse exploratory nature of the Materials Laboratory effort. To meet these needs effectively, the program was performed on-site at the AFWAL Materials Laboratory.

The staff assigned to this effort included:

Project Manager/Principal Investigator	A. G. Jackson, Ph.D.
Assistant Project Manager/TEM/STEM	R. E. Omlor, BS
Analytical Electron Microscopy	A. G. Jackson, Ph.D.
Microtomy/TEM/STEM	P. F. Lloyd/S. D. Apt, BA
SEM	R. J. Bacon, AD/R. D. Brodecki
EPMA	R. J. Bacon, AD/ A. G. Jackson, Ph.D.
Metallography Lab	C. E. Harper/F. O. Deutscher/ R. K. Lewis
Photo Lab	J. C. Heidenreich/S. D. Apt, BA
Special Projects	J. G. Paine
Technical Support	J. S. Paine

Their conscientious effort in producing high-quality data and analyses is gratefully acknowledged.

## SECTION 2

### SUMMARY OF WORK PERFORMED

#### ELECTRON OPTICS

Characterization research performed using electron-optical methods resulted in a number of papers and presentations as listed in Section 3. Since these papers and presentations have appeared in the open literature, the reader is referred to the appropriate sources for details.

During the period of the contract, the electron-optics instrumentation was upgraded by the replacement of the JEOL 200A TEM with a JEOL 2000FX STEM with Tracor-Northern 5500 energy-dispersive spectroscopy and Gatan energy-loss spectrometer. These instruments add considerably to the capability for quantitative analyses of phases and identification of the crystallography present in materials being studied, particularly through use of convergent-beam diffraction analyses. In addition, a Gatan scanning ion mill used for precision milling of TEM foils was installed, allowing improved specimen preparation of difficult-to-polish specimens such as ceramics and non-disc-shaped foils such as wires and fibers.

Electron-microprobe research was hindered because of the deteriorating condition of the ETEC autoprobe instrument. Replacement parts were difficult to obtain, and service support from ETEC essentially ceased. This situation was recognized by the Materials Laboratory, and a replacement SEM/PROBE was obtained. The JEOL 844 instrument with the Tracor-Northern 5600 automation package and six-crystal spectrometer system arrived in late spring of 1986 and was completely installed by August 31, 1986. Resolution in the SEM using a tungsten filament is about 4.0 nm and has been verified using resolution standards.

Statistics for efforts in each of the electron-optics areas during this contract are as follows:

### TEM/STEM

	<u>Number of specimens</u>
TEM and SEM Sample Preparation	187
Electropolished	1,791
	<u>Number of photoplates</u>
Ion Milled	2,461
2000 FX	2,890
100 CX	27,695
	<u>Number of spectra analyzed</u>
EDS	107

### SEM

During this period 2,457 samples were examined, requiring 11,723 photographs with negatives. Color photographs and DecWriter printouts of EDS analysis spectra were also obtained.

### EPMA

Quantitative data were obtained on 2,540 samples submitted during this contract.

### AEM

Research on the microstructure, morphology, and crystallography of the alloys using AEM techniques was initiated during this contract. Specific methods employed included quantitative composition analyses using energy dispersive and energy-loss spectroscopy. Concerted efforts were made to apply convergent-beam electron diffraction to the determination of phases present in rapidly solidified alloys; the result was development of refinements to analysis techniques (see publication list). Unpublished results from three projects are documented herein. In most cases the information is useful but not sufficiently complete for publication.

A detailed characterization of the operation of the energy-loss spectrometer was initiated to determine the optimum conditions for collecting the loss signal. The result of the research was that use of the convergent-beam diffraction mode on the 2000FX instrument provided the optimum signal to noise but not necessarily the optimum resolution. The effects of using image or diffraction-pattern modes for collecting the signal were explored. The fine structure in the post-excitation spectrum is affected by the mode employed as well as the orientation of the specimen with respect to the beam. These are well-known effects, but the specific effects in the 2000FX instrument required examination. This project was not complete at the end of this contract, and further research is needed. The Tracor-Northern program for energy loss works well for a single spectrum, but does not function reliably for acquisition of multiple spectra. Discussions with Tracor-Northern have helped in seeking a solution to this problem, but the difficulty has not been resolved.

#### Analysis of Al-Ho Alloy

Diffraction patterns from a foil of Al-Ho (RST) were obtained in an effort to identify the compound present. Two types of precipitate were observed--Type 1 was in a very thin section, probably oxidized, and Type 2 was in a thicker section of the foil and had a different shape. Type 1 appeared to have a eutectic morphology in the form of irregular shapes; Type 2 was more spheroidal in shape. Five compounds of Al-Ho have been documented in the literature (Table 1). For the foil under examination, the compound was  $\text{Al}_3\text{Ho}$  since the foil had been heat-treated at  $450^\circ\text{C}$  for several hours in order to coarsen any precipitates present. Earlier examination of this foil by EDS showed Ho in the matrix in Types 1 and 2, although the phase diagram indicates no solubility of Ho in Al.

Experimental Results. A diffraction pattern from Type 1 ppts is shown in Fig. 1. The diffuse background originated in the matrix as determined by moving the specimen to several locations. The fine spots present in the figure changed as the specimen was moved, while the diffuse rings remained constant.



The measured radius of the ring was 8.61 mm (or  $2.87 \pm 0.05 \text{ \AA}$ ). The measured radii of the major spots were  $7.88 \pm 0.1$ ,  $8.15 \pm 0.1$  mm,  $8.33 \pm 0.1$  mm (or  $3.13 \pm 0.04 \text{ \AA}$ ,  $3.03 \pm 0.04 \text{ \AA}$ , and  $2.97 \pm 0.04 \text{ \AA}$ ). Measurements were made on an enlarged print; distances on the print were converted to Angstrom units by using a calibrated magnification factor and the known value of the camera constant (5.46 and  $24.7 \text{ mm-\AA}$ ).

TABLE 1  
DOCUMENTED COMPOUNDS OF Al-Ho

COMPOUND	LATTICE PARAMETERS			CRYSTAL TYPE
	a	b	c	
HoAl <sub>3</sub>	12.44	$28.13 \pm \alpha$	-	RHO
	6.050	35.82	-	HLP
HoAl <sub>2</sub>	7.814	-	-	CUB
HoAl	5.801	11.34	5.621	ORT
Ho <sub>3</sub> Al <sub>2</sub>	8.182	7.541	-	TET
Ho <sub>2</sub> Al	6.528	5.053	9.347	ORT

1-5: increasing Ho

Eutectic at 11 w/o, 65°C



Figure 1. Diffraction Pattern from Al-Ho.

The value for the diffuse ring ( $2.87 \pm 0.05 \text{ \AA}$ ) does not correspond to any plane in  $\text{Al}_2\text{O}_3$  (see Table 2), suggesting a different form of  $\text{Al}_2\text{O}_3$  produced by the presence of Ho. Such an impurity-stabilized form is evidently common in the  $\text{Al}_2\text{O}_3$  impurity system.

The distances measured for the spots in the pattern showed no correlation with the expected Al-Ho compounds. Tables 3, 4 and 5 give planes and interplanar separations for  $\text{HoAl}_3$ ,  $\text{HoAl}_2$ , and  $\text{HoAl}$ , respectively. While individual planes from each compound fit, no single compound fits the data. These results are summarized in Table 6.

The bright-field and diffraction patterns from Type 2 ppt and matrix are shown in Fig. 2. Analysis of the matrix revealed the zone to be  $[\bar{1}12]\text{-Al}$ . These data are summarized in Table 7. The error present in the ratios suggests that some distortion may be present in the matrix, probably because of the presence of Ho. The atomic radius of Ho is  $1.58 \text{ \AA}$ , while that of Al is  $1.18 \text{ \AA}$ . Hence, if Ho is substitutionally present in solution, lattice distortions would be expected--particularly in the close packed plane (111).

Attempts to analyze the diffraction pattern from the ppt were not successful. No planes and angles fit the data from  $\text{HoAl}_3$ ,  $\text{HoAl}_2$ , or  $\text{HoAl}$ . These data are summarized in Table 8.

Conclusions The foil contains two types of precipitate compounds, and Ho is in solution in the Al matrix. The presence of distortions to the Al lattice is probably due to the large mismatch between the atomic radii of Ho and Al. Further analysis using new patterns and additional EDS data will be required for identification of the compound.

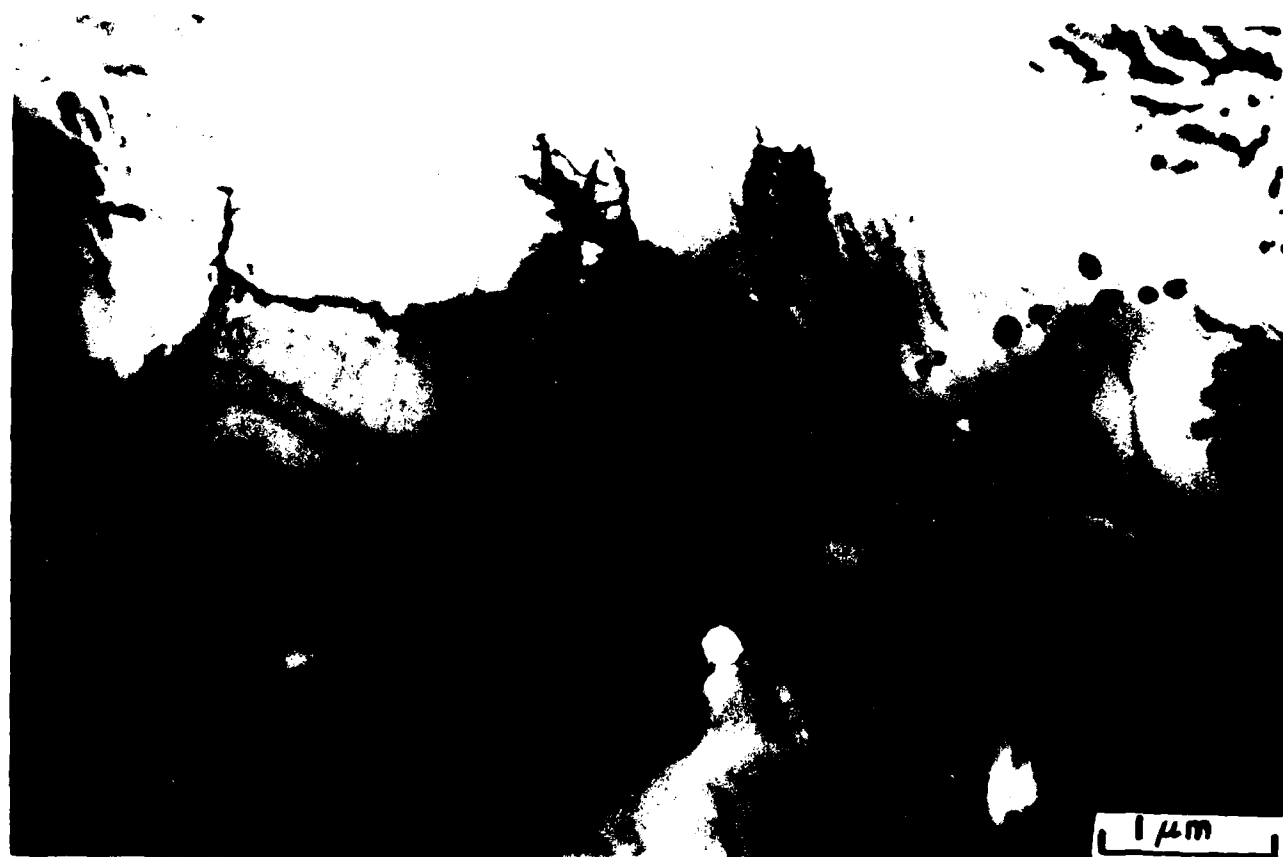


Figure 2(a). Bright Field of Grains in Al-Ho.

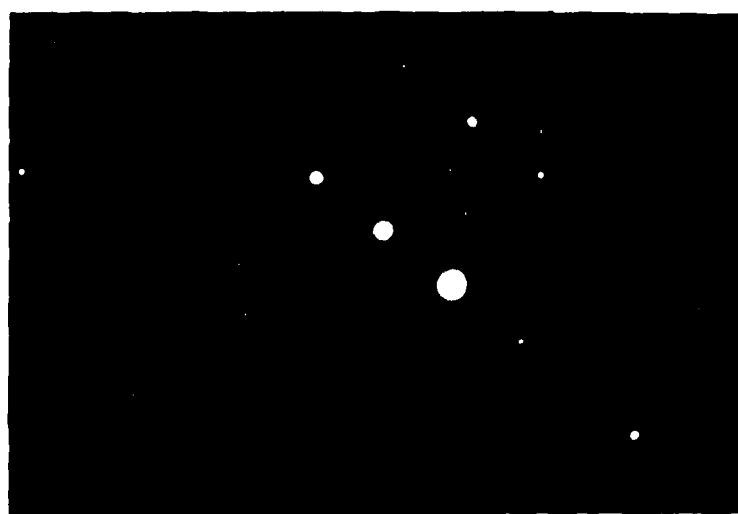


Figure 2(b). Diffraction Pattern from Area in 2(a).

TABLE 2

PLANES AND INTERPLANAR SEPARATIONS FOR  $\text{Al}_2\text{O}_3$   
 (LATTICE CONSTANTS ARE 3.1, 0, 4.99)

1	0.493	(3,3,-6,3)
3	0.505	(3,3,-6,2)
4	0.513	(3,3,-6,1)
5	0.516	(3,3,-6,0)
6	0.577	(3,2,-5,3)
7	0.597	(3,2,-5,2)
8	0.611	(3,2,-5,2)
9	0.615	(3,2,-5,0)
10	0.679	(3,1,-4,3)
11	0.702	(2,2,-4,3)
12	0.713	(3,1,0,4,2)
13	0.736	(3,1,-4,1)
14	0.740	(2,2,-4,2)
15	0.744	(3,1,-4,0)
16	0.765	(2,2,-4,1)
17	0.775	(2,2,-4,0)
18	0.788	(3,0,-3,3)
19	0.842	(3,0,-3,2)
20	0.866	(3,-1,-2,3)
21	0.880	(3,0,-3,1)
22	0.894	(3,0,-3,0)
23	0.939	(3,-1,-2,2)
24	0.994	(3,-1,-2,1)
25	1.01	(3,-1,-2,0)
26	1.04	(2,0,-2,3)
27	1.13	(2,-1,-1,3)
28	1.18	(2,0,-2,2)
29	1.29	(2,0,-2,1)
30	1.31	(2,-1,-1,2)
31	1.34	(2,0,-2,0)
32	1.41	(1,0,-1,3)
33	1.48	(2,-1,-1,1)
34	1.55	(2,-1,-1,0)
35	1.66	(0,0,0,3)
36	1.82	(1,0,-1,2)
37	2.36	(1,0,-1,1)
38	2.49	(0,0,0,2)
39	2.68	(1,0,-1,0)
40	4.99	(0,0,0,1)

TABLE 3

PLANES AND INTERPLANAR SEPARATIONS FOR  $\text{HoAl}_3$   
(LATTICE CONSTANTS ARE 6.05, 0, 35.82)

1	1.004	(3,3,-6,3)
3	1.006	(3,3,-6,2)
4	1.007	(3,3,-6,1)
5	1.008	(3,3,-6,0)
6	1.195	(3,2,-5,3)
7	1.199	(3,2,-5,2)
8	1.201	(3,2,-5,1)
9	1.202	(3,2,-5,0)
10	1.442	(3,1,-4,3)
11	1.448	(3,1,-4,2)
12	1.451	(3,1,-4,1)
13	1.453	(3,1,-4,0)
14	1.500	(2,2,-4,3)
15	1.507	(2,2,-4,2)
16	1.511	(2,2,-4,1)
17	1.512	(2,2,-4,0)
18	1.728	(3,0,-3,3)
19	1.738	(3,0,-3,2)
20	1.744	(3,0,-3,1)
21	1.746	(3,0,-3,0)
22	1.953	(3,-1,-2,3)
23	1.968	(3,-1,-2,2)
24	1.977	(3,-1,-2,1)
25	1.980	(3,-1,-2,0)
26	2.558	(2,0,-2,3)
27	2.592	(2,0,-2,2)
28	2.612	(2,0,-2,1)
29	2.619	(2,0,-2,0)
30	2.932	(2,-1,-1,3)
31	2.982	(2,-1,-1,2)
32	2.0±3	(2,-1,-1,1)
33	3.025	(2,-1,-1,0)
34	4.797	(1,0,-1,3)
35	5.028	(1,0,-1,2)
36	6.184	(1,0,-1,1)
37	5.239	(1,0,-1,0)
38	11.94	(0,0,0,3)
39	17.91	(0,0,0,2)
40	35.82	(0,0,0,1)

TABLE 4

PLANES AND INTERPLANAR SEPARATIONS FOR  $\text{HoAl}_2$   
(LATTICE CONSTANTS ARE 7.814, 0, 0)

1	1.503	(3,3,3)
3	1.665	(3,3,2)
4	1.792	(3,3,1)
5	1.841	(3,3,0)
6	1.895	(3,2,2)
7	2.088	(3,2,1)
8	2.167	(3,2,0)
9	2.255	(2,2,2)
10	2.356	(3,1,1)
11	2.471	(3,1,0)
12	2.604	(3,0,0)
13	2.762	(2,2,0)
14	3.190	(2,1,1)
15	3.494	(2,1,0)
16	3.907	(2,0,0)
17	4.511	(1,1,1)
18	5.525	(1,1,0)
19	7.814	(1,0,0)

TABLE 5

PLANES AND INTERPLANAR SEPARATIONS FOR  $\text{HoAl}$   
(LATTICE CONSTANTS ARE 5.801, 11.34, 5.621)

1	1.267	(3,3,3)
3	1.309	(3,2,3)
4	1.336	(3,1,3)
5	1.345	(3,0,3)
6	1.452	(2,3,3)
7	1.467	(3,3,2)
8	1.516	(2,2,3)
9	1.533	(3,2,2)
10	1.558	(2,1,3)
11	1.573	(2,0,3)
12	1.577	(3,1,2)
13	1.593	(3,0,2)
14	1.612	(1,3,3)
15	1.676	(3,3,1)
16	1.678	(0,3,3)
17	1.700	(1,2,3)
18	1.721	(3,3,0)
19	1.740	(3,2,1)
20	1.761	(1,1,3)
21	1.779	(0,2,3)
22	1.780	(2,3,2)
23	1.782	(1,0,3)

TABLE 5 (Continued)

24	1.805	(3,1,1)
25	1.828	(3,0,1)
26	1.830	(3,2,0)
27	1.848	(0,1,3)
28	1.873	(0,0,3)
29	1.901	(2,2,2)
30	1.906	(3,1,0)
31	1.933	(3,0,0)
32	1.987	(2,1,2)
33	2.018	(2,0,2)
34	2.102	(1,3,2)
35	2.129	(2,3,1)
36	2.255	(0,3,2)
37	2.301	(2,3,0)
38	2.309	(1,2,2)
39	2.346	(2,2,1)
40	2.468	(1,1,2)
41	2.513	(2,1,1)
42	2.518	(0,2,2)
43	2.529	(1,0,2)
44	2.577	(2,0,1)
45	2.582	(2,2,0)
46	2.727	(0,1,2)
47	2.759	(1,3,1)
48	2.810	(2,1,0)
49	2.810	(0,0,2)
50	2.900	(2,0,0)
51	3.136	(0,3,1)
52	3.166	(1,3,0)
53	3.288	(1,2,1)
54	3.78	(0,3,0)
55	3.803	(1,1,1)
56	3.991	(0,2,1)
57	4.036	(1,0,1)
58	4.054	(1,2,0)
59	5.036	(0,1,1)
60	5.164	(1,1,0)
61	5.621	(0,0,1)
62	5.67	(0,2,0)
63	5.801	(1,0,0)
64	11.34	(0,1,0)

TABLE 6  
COMPARISON OF MEASURED AND  
CALCULATED DISTANCES IN SEVERAL COMPOUNDS

		<u>Measured</u>	<u>Plane</u>	<u>Compound</u>
Diffuse Ring		$2.87 \pm 0.05 \text{ \AA}$	-	none
Spots	1	3.13   3.14	031	HoAl
	2	3.03   3.02	2 $\bar{1}\bar{1}$ 1	HoAl <sub>3</sub>
		3.03	2 $\bar{1}\bar{1}$ 0	
	3	2.97   2.98	2 $\bar{1}\bar{1}$ 2	HoAl <sub>3</sub>
		$\pm 0.04$		

TABLE 7  
ANALYSIS OF Al MATRIX DIFFRACTION PATTERN  
(Plate 21731)  
(Camera Constant = 24.7)

<u>Spot</u>	<u>R</u>	<u>d</u>	<u>Plane</u>	<u>d<sub>Th</sub></u>
1	10.7	2.31	111	2.338
2	20.25	1.22	113	1.221
3	17.25	1.43	220	1.432
4	20.25	1.22		(a = 4.04)

<u>Angles</u>	<u>Meas.</u>	<u>Theor.</u>
1-2	58.4	58.5
2-3	31.9	31.5

<u>Ratios</u>	<u>Meas.</u>	<u>Planes</u>	<u>Theor.</u>	<u><math>\Delta</math> (Å)</u>	<u>%</u>
1:2	1.89	111/113	1.92	-0.03	-1.56
3:2	1.17	220/113	1.17	0.0	0
1:3	1.61	111/220	1.63	-0.02	-1.24



TABLE 8  
ANALYSIS OF PRECIPITATE DIFFRACTION PATTERN

<u>Spot</u>	<u>R</u>	<u>d</u>	<u>Angles</u>	<u>Meas.</u>
1	4.5	5.49	1-2	66.6
2	6	4.12	2-3	44.4
3	5.9	4.19		

#### Literature Review of Ti-6Al-4V

Several studies of the physical metallurgy of Ti-6Al-4V have been documented during the last 25 years. These have been concerned mainly with (1) the microstructure produced by heat treatments in the  $\beta$  and  $\alpha + \beta$  phase fields and (2) the transformations occurring in this system. The results of these studies are summarized below.

Imam and Gilmore<sup>1</sup> studied the effect of aging on the microstructure of Ti-6-4V. Specimens annealed at 1300°F for 2 hr. were heated to 1652°F for 10 min. and then water quenched, resulting in  $\alpha + (\alpha' + \beta)$  with a distribution of 50%  $\alpha$ , 25%  $\alpha'$  and 25%  $\beta$ . Aging at 932°F for 1 hr. resulted in growth of  $\alpha'$  at the expense of  $\beta$ . Aging at the same temperature for 8 hr. resulted in loss of all  $\beta$ . Quenching the specimen from 1949°F yielded 100%  $\alpha'$ . The  $\beta$  produced at the lower temperature quench (1652°F) was richer in V than the transformed- $\beta$  produced at the higher temperature (1949°F). The lower-temperature  $\beta$  is more stable because of the higher V content. The  $\beta$  present in the 1652°F quenched alloy underwent an isothermal transformation to  $\alpha'$ .

Murakami<sup>2</sup> reviewed the transformations observed in Ti alloys and tabulated his results for quick reference. For  $\alpha + \beta$  alloys such as Ti-6-4 the transformations are:

$(\beta > \alpha', \alpha'', \omega \text{ (athermal)} + \beta \text{ on quenching, } \alpha'' + \beta.$

$\beta > \alpha', \alpha'', \omega \text{ (athermal)} + \beta \text{ on quenching, } \alpha'' + \beta.$

$\beta \text{ (lean)} > \alpha'' \text{ (lean)} + \alpha'' \text{ (rich)} > \alpha'' \text{ (lean)} + \beta > \alpha + \beta$

Chestnutt, Rhodes, and Williams<sup>3</sup> discussed Ti-alloy transformations and presented their definitions of the many types of microstructures appearing

in these alloys. They pointed out that in lean- $\beta$ -stabilized alloys (e.g., Ti-6Al-4V), it is difficult to form  $\alpha'$  fully, since the kinetics for  $\alpha$ -phase formation are sufficient for successful competition with  $\alpha'$  formation. Thus, in Ti-6Al-4V  $\alpha$  is present at preferred nucleation sites such as prior- $\beta$  grain boundaries. The type of  $\alpha$  produced by heat treatment varies, depending on solute content and rate of cooling. A slow cool or lean- $\beta$  content yields Widmanstätten- $\alpha$  colonies with the same variant present. Rapid cooling or high  $\beta$  content results in nucleation and growth of other variants of  $\alpha$ . Thus, two types of  $\alpha$  may be produced.

Williams and Hickman<sup>4</sup> discussed tempering in Ti alloys and pointed out that in Ti-6Al-4V tempering occurs by precipitation of  $\beta$  which reduces the supersaturation present in the  $\alpha'$ , yielding equilibrium. However, if  $\alpha''$  forms, this sequence does not occur. In this case  $\alpha$  precipitates first, yielding an enriched  $\alpha''$ , which must subsequently decompose to  $\beta$ .

McQuillan<sup>5</sup> in an early review of Ti-alloy transformations pointed out that in Ti-6Al-4V,  $\beta$  is not retained upon quenching if the temperature is above 1382°F. The second martensite was not  $\alpha''$  but a structure having a slightly different  $c$  value. Aging of Ti-6Al-4V yielded three hardness peaks--the first due to precipitation, the second unexplained, and the third due to enrichment of  $\beta$ . No  $\omega$  phase was reported.

In a detailed study of Ti-6Al-4V reported by Fopiano, Bever, and Averbach,<sup>6</sup> a range of solution-treatment temperatures was applied. Phases present were:  $\alpha + \beta$  below 1382°F;  $\alpha'$  above 1472°F; no  $\beta$  between 1562 and 1742°F;  $\alpha'$  only at 1832°F. All specimens were held at temperature for 1 hr. and then water quenched.

Decomposition of  $\beta$  phase upon aging proceeds thusly: the slower the rate, the higher the solution treatment. Aging time for appearance of  $\beta$  X-ray lines was 15 min. at 1000°F for the specimen solution treated at 1562°F, while  $\beta$  appeared after 12 hr. at 2000°F for the specimens treated at 1742°F. The relative diffusivities of V and Al were estimated, and an activation energy of 45 kcal/mole was found for Al in Ti. V diffuses faster than Al in Ti. The decomposition energy for  $\alpha'$  was determined to be  $\sim 14$  kcal/atom. The  $\gamma$  ( $\text{Ti}_3\text{Al}$ ) phase may form.  $\alpha + \beta$  was found at 1382°F;

at 1562°F,  $\alpha + \alpha''$  was found; at 1742°F,  $\alpha + \alpha' +$  unknown phase at  $\alpha/\alpha'$  interface was found. Aging of the specimen at 1000°F and solution treating at 1562°F yielded  $\alpha + \alpha' > \alpha + (\alpha + \beta) > \alpha + \gamma + \beta$ .

Seagle and Bartlo<sup>7</sup> reported the microstructures produced in Ti-6Al-4V for water quench, air cool, and furnace cool from three temperatures. Their results are listed in Table 9.

TABLE 9  
MICROSTRUCTURES OBSERVED IN Ti-6Al-4V FOR VARIOUS TYPES OF QUENCH

QUENCH TEMP. (°F)	QUENCH TYPE		
	WATER	AIR COOL	FURNACE COOL
1950	$\alpha'$	$\alpha(\text{acic})$	$\alpha(\text{plate})$
1750	$\alpha(p) + \alpha'$	$\alpha + \alpha(T)$	$\alpha(\text{eq}) + \beta(\text{int})$
1550	$\alpha(p) + \beta$ (ret)	$\alpha + \alpha'$	$\alpha(\text{eq}) + \beta(\text{int})$

$\alpha' =$  transformed  $\beta$

$\alpha(T) =$  transformed  $\beta$

$\alpha(\text{acic}) =$  acicular  $\alpha$

$\alpha(\text{eq}) =$  equilibrium  $\alpha$

$\alpha(\text{plate}) =$  platelike  $\alpha$

$\beta(\text{ret}) =$  retained  $\beta$

$\alpha(p) =$  primary  $\alpha$

$\beta(\text{int}) =$  intergranular  $\beta$

Dyakova, et. al.<sup>8</sup>, used a Ti-Al-V alloy, but the exact composition was not given. The martensite start temperature ( $M_s$ ) listed was 572 - 662°F--very low in comparison with other values for Ti-6Al-4V which probably indicates a high V content since this will lower the  $M_s$  according to Ref. 9. For the Ti-6Al-4V alloy,  $\alpha''$  forms upon quenching from 900°C (1652°F). If the quench is to a temperature below the  $M_s$ , then the  $\alpha''$  decomposes to a V-poor  $\alpha''$  and an enriched  $\alpha''$ , in which the  $\alpha$  forms first, followed by nucleation of  $\beta$  phase in the enriched  $\alpha''$ . The final decomposition products are  $\alpha$  and enriched  $\beta$ . If the quench is accomplished to a temperature above the  $M_s$ , then the  $\beta$  decomposes by a diffusional mechanism according to free-energy considerations. In zones poor in  $\beta$  stabilizer (low in V), the  $\beta$  transforms to  $\alpha''$ . The maximum  $\beta$  decomposition occurs at 550°C (1022°F) and yields  $\alpha + \beta$ .

In Rhodes and Williams<sup>10</sup> the  $\alpha/\beta$  interface phase in Ti-6Al-4V is Type-2  $\alpha$  and has a densely striated layer originating at the  $\alpha/\beta$  boundary which grows into the  $\alpha$ . The phase arises when  $dT/dt = 900^\circ\text{C/hr}$  and starts high in the  $\beta$  phase. If  $dT/dt = 100^\circ\text{C/hr}$  and the same starting phase as above is present, then no interface phase is generated. Instead a monolithic phase (FCC) is generated ( $a = 4.22 \text{ \AA}$ ).

The results of Rhodes and Paton<sup>11</sup> for Ti-6Al-4V concerning the interface phase are as follows for a quench rate fixed at  $38^\circ\text{C/hr}$ :

- (1) Heat at  $980^\circ\text{C}/2 \text{ hr.}$ , quench to  $760^\circ\text{C}$  ( $1400^\circ\text{F}$ ), WQ: interface phase, FCC.
- (2) Heat at  $980^\circ\text{C}/2 \text{ hr.}$ , quench to  $20^\circ\text{C}$ , WQ: striated layer (Type-2  $\alpha$ ).
- (3) Heat at  $925^\circ\text{C}/2 \text{ hr.}$ , quench to  $650^\circ\text{C}$  ( $1202^\circ\text{F}$ ), WQ: striated layer present;
- (4) Heat at  $925^\circ\text{C}/2 \text{ hr.}$ , quench to  $870^\circ\text{C}$  ( $1598^\circ\text{F}$ ), WQ: no layer present.

These authors also note that the change of volume upon transforming from  $\beta$  to  $\alpha$  is about + 5%.

In Welsch, et. al.,<sup>12</sup>  $\beta$  transforms to  $\alpha'$  and then to  $\alpha + \beta$  if quenched from a temperature greater than  $800^\circ\text{C}$  ( $1472^\circ\text{F}$ ).  $\beta$  transforms to  $\alpha + \beta$  if quenched from a temperature lower than  $800^\circ\text{C}$  in the case of highly enriched  $\beta$  or upon slow cooling. A quench from  $810^\circ\text{C}$  and WQ yields 90%  $\alpha$  and 10%  $\alpha''$  and  $\beta$ , which subsequently decomposes to  $\alpha$  and  $\beta$  upon aging at  $550^\circ\text{C}$ . Also  $\alpha''$  forms ( $\text{Ti}_3\text{Al}$ ) in the primary- $\alpha$  grains. The decomposition of  $\beta$  to  $\alpha$  and  $\beta$  is approximately even, i.e., 5%  $\alpha$  and 5%  $\beta$ .

Studies of the ternary phase diagram for Ti-Al-V were conducted by Farrar and Margolin.<sup>13</sup> The temperature range covered by their work was 1112 to  $2552^\circ\text{F}$ . Examination of isothermal sections for  $180^\circ\text{F}$  increments reveals that the phases present in Ti-6Al-4V at the lower temperatures include  $\alpha$ ,  $\beta$ ,  $\gamma$  and possibly  $\Delta$ . Phases of interest here are HCP  $\alpha$ , BCC  $\beta$ ,  $\gamma$  ( $\text{Ti}_3\text{Al}$ ), and  $\sigma$  ( $\text{Ti}_2\text{Al}$ ).

## Ti-6Al-4V Phase Diagram

Many pseudo-binary Ti-V diagrams for Ti-6Al-4V have been offered, but their usefulness is limited to trend indications which are valuable for qualitative understanding of gross behavior. For Ti-6Al-4V such a diagram is given in Fig. 3, which was constructed from data of Fopiano, Bever, and Averbach.<sup>6</sup> The two-phase field extends from at least 1300 to 1830°F and includes the 4 w/o content of the alloy. At what point the alloy becomes single phase at lower temperature is not clear. Based on this diagram, heat treatment at high temperature, near the  $\beta$  transus, is expected to yield  $\beta$  phase with V content near 4 w/o. As the heat treatment temperature decreases, the expected V content in  $\beta$  increases, leading to a  $\beta$ -stabilized phase.

Transformation of  $\beta$  to  $\alpha'$  occurs when the heat treatment temperature is above the  $M_s$  temperature. Estimates of this temperature vary widely, but it does not appear to be higher than the  $T_0$  line estimated by drawing the locus of the bisector of the two-phase region.

Curves for  $M_s$  as a function of alloy and content have been reported by Huang, *et al.*,<sup>14</sup> for alloys of Ti with a number of solutes. This curve for Ti-V has been plotted in Fig 3. If the plots of  $M_s$  vs. solute w/o for Ti-V and Ti-Al are combined, assuming Al solute w/o to be constant, the resulting  $M_s$  curves are above those of the binary.

Determination of the  $M_s$  temperature as a function of V content has not been reported for the ternary alloy; but Fopiano, Bever, and Averbach<sup>3</sup> list the  $M_s$  for various solution treatments in which the V content of the  $\beta$  phase varied from about 4 w/o to 14 w/o. The  $M_s$  in the binary Ti-X system where X is a metal has been published (based on thermodynamic data) by Huang, Suzuki, Kaneko, and Sato.<sup>14</sup> The curve shows that for small amounts of Al, the  $M_s$  is relatively constant but the  $M_s$  drops markedly for increasing V content, reaching 572°F for 12.5 w/o V. Experimentally, the type of behavior indicated in this diagram has been reported. While additional phases such as  $\gamma$  or  $\alpha''$  (orthorhombic martensite) do not appear on the diagram, they have been observed in Ti-6Al-4V.<sup>15,16</sup>

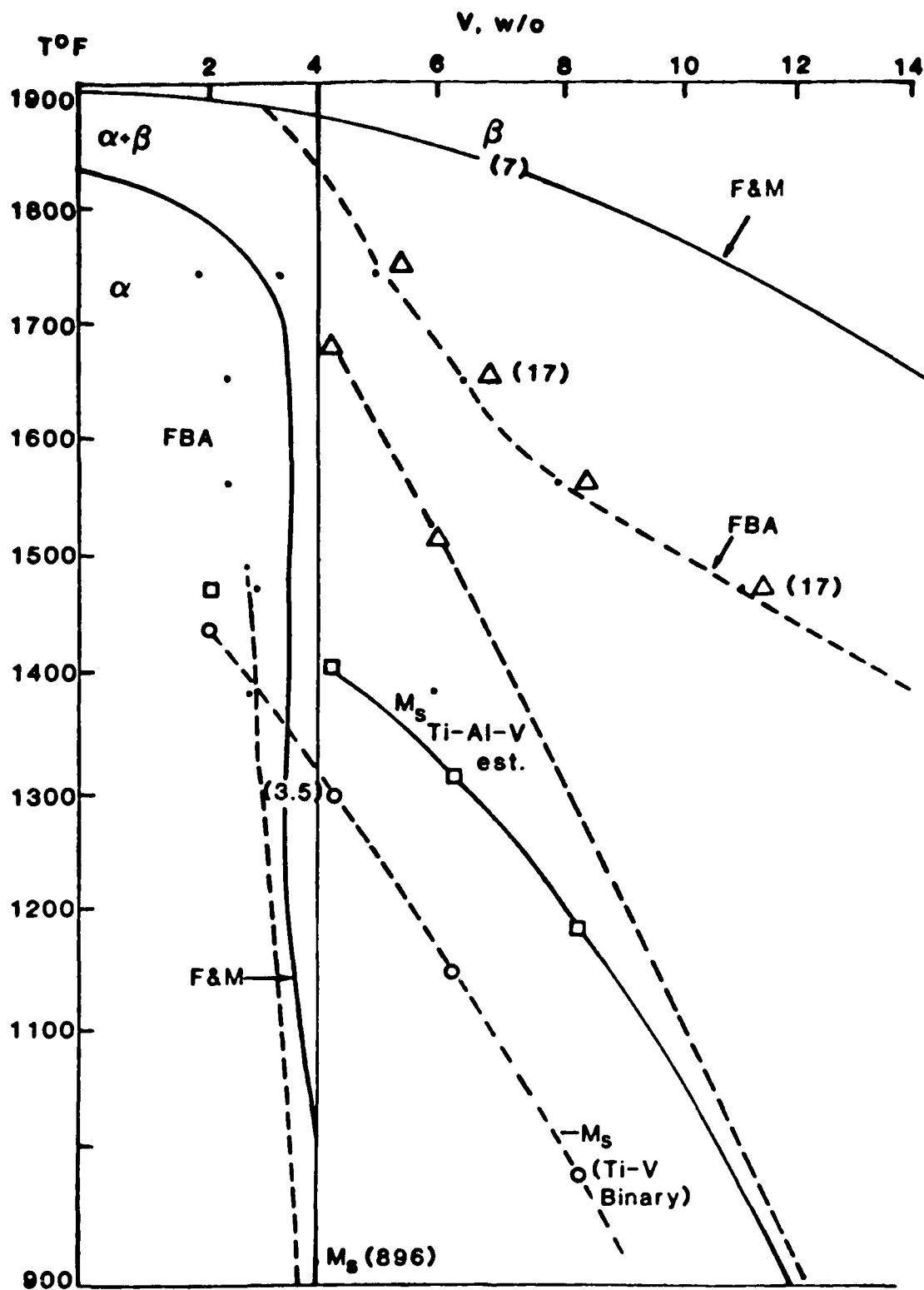


Figure 3. Ti-6Al-4V Pseudo-Binary Phase Diagram. FBA = Fopiano, Bever, and Averbach;<sup>6</sup> F&M = Farrar and Margolin;<sup>13</sup>  $M_s$  Ti-V Binary Data = Huang, et al.<sup>14</sup>

An estimate of the binary phase diagram was obtained from the ternary diagrams of Farrar and Margolin.<sup>13</sup> The transi differ from those of Fopiano, Bever, and Averback,<sup>6</sup> particularly for the  $\beta$  transus.

Figure 4 was constructed by noting the transi present based on the ternary diagrams, assuming a constant 6 w/o Al. This plot includes not only  $\alpha$  and  $\beta$  but also  $\gamma$  and  $\Delta$ --particularly in the temperature range below 1472°F. Ti-6Al-4V falls well within the  $\alpha$  and  $\alpha + \beta$  phase fields, but  $\alpha + \gamma$  is possible at temperatures below 1472°F. The  $\gamma$  phase has been reported by Welsch, et al.,<sup>12</sup> for annealing and quenching from 1490°F followed by aging at 1022°F, the  $\gamma$  precipitating from the primary  $\alpha$ . Fopiano, Bever, and Averback<sup>6</sup> also obtained  $\gamma$  after solution treatment at 1562°F and WQ, followed by aging at 1000°F, although the precursor to  $\gamma$  was not identified. These results are consistent with the ternary based binary diagram.

Volume Fraction of  $\beta$  as Function of Temperature. Fopiano, et al.,<sup>6</sup> present volume-fraction data for various temperatures; the data are plotted in Fig. 5. The behavior at  $T < 1382^\circ\text{F}$  is uncertain since this is the lowest temperature reported. The composition of the  $\alpha$  and  $\beta$  is reported for each temperature of value in constructing a phase diagram and understanding more clearly the enrichment of  $\beta$  possible by treatment at temperatures low relative to the  $\beta$  transus.

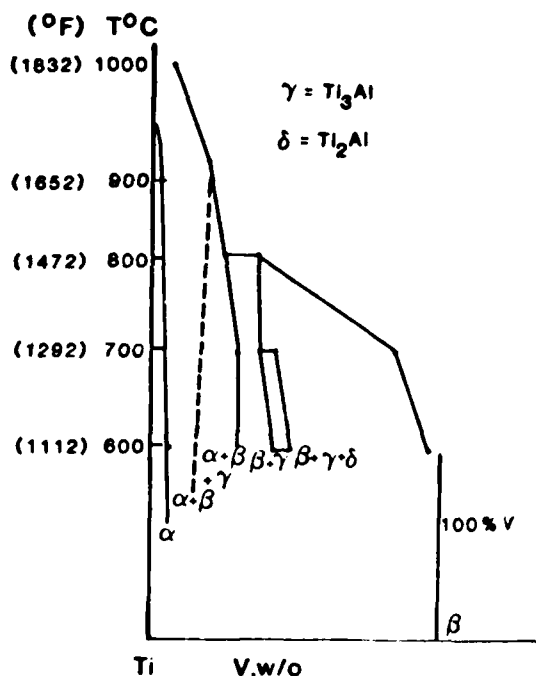


Figure 4. Ti-V Binary Diagram Extrapolated from Ternary Data of Farrar and Margolin.<sup>13</sup>

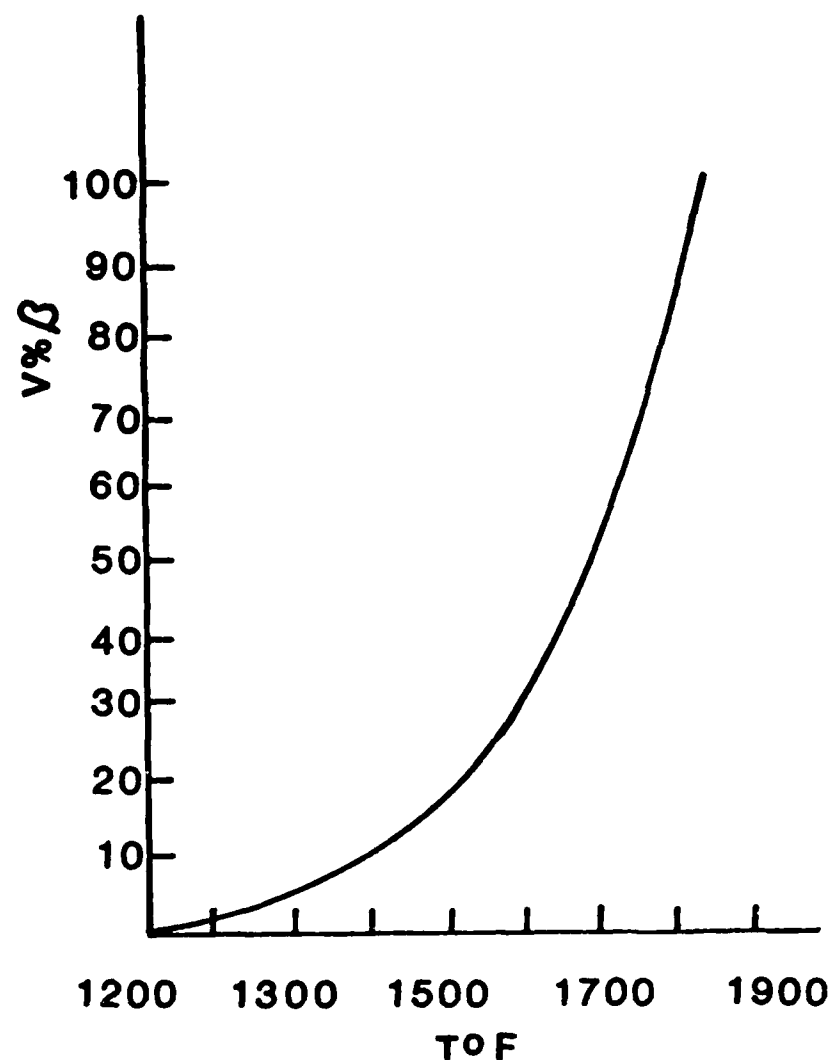


Figure 5. Volume Fraction of  $\beta$  as Function of Temperature (from Fopiano, Bever, and Averbach<sup>6</sup>).

Maximum-Lathe-Size Measurement. Measurements of the maximum lathe size observed in Ti-6Al-4V powder were made from micrographs of a range of powder diameters. The purpose of this measurement was to determine whether any relationship exists between the  $\beta$  grain size and the largest lathe size present.

The minimum lathe size and  $\beta$  grain size are plotted in Fig. 6 as a function of particle size. From the plot the lathe size appears to be limited by grain size for particle diameters of 150  $\mu$  or less. Above this diameter the curves diverge, the lathe size being smaller than the grain size.



V-Diffusion Calculations Using an equation for V diffusion in Ti developed by Murdock,<sup>17</sup> distances diffused at various temperatures and times were calculated (see Fig. 7). The purpose of the calculation was to obtain estimates of movement of V in Ti-6Al-4V in order to assess potential  $\alpha$  or  $\beta$  phase formation requiring mass transfer.

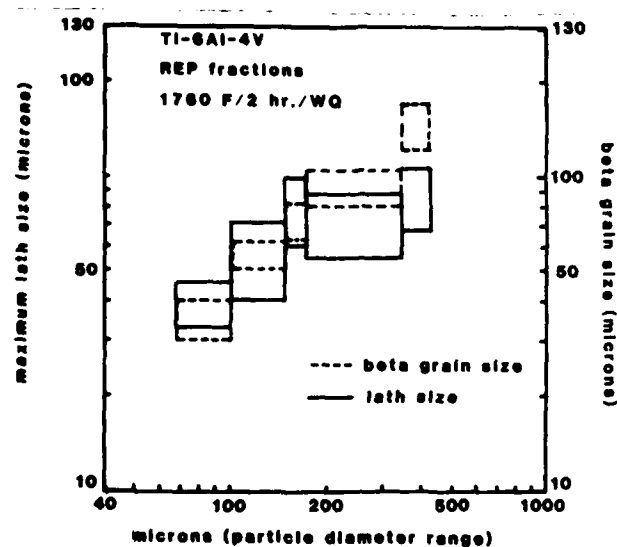


Figure 6. Plot of Maximum Lath Size vs Particle Size for Ti-6Al-4V Powder.<sup>18</sup>

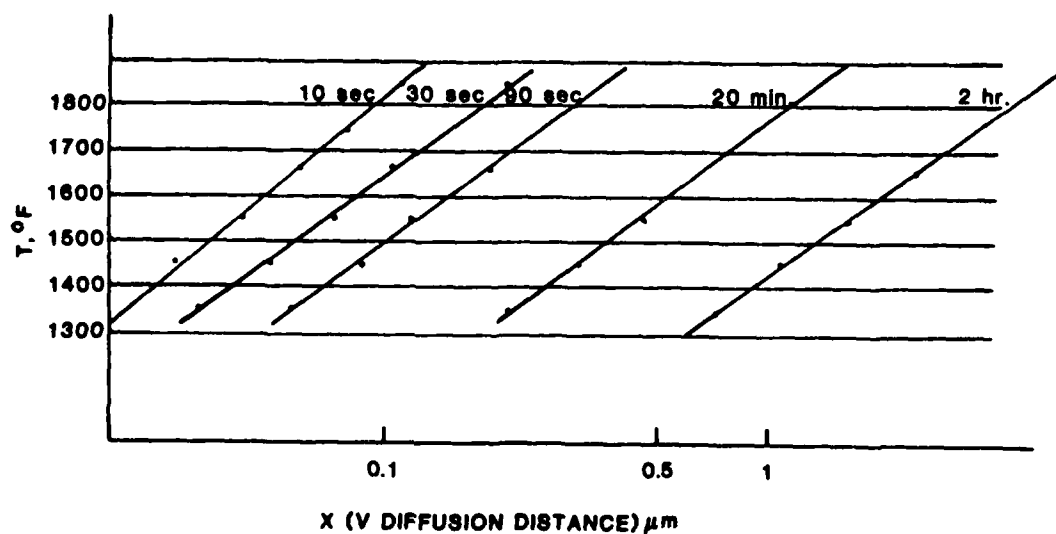


Figure 7. Distance Diffused for V in Ti for Various Temperatures and Times.

The plots show that movement of V for distances large compared with the  $\beta$  grain size (10-100  $\mu\text{m}$ ) is not expected in times of less than a few hours if the morphology consists only of  $\beta$  grain boundaries. The presence of martensite plates, however, complicates the predictions since diffusion along martensite/martensite interfaces may be more rapid than indicated by bulk calculations.

V diffusion is estimated to be more rapid than Al diffusion. If boundaries are the preferred sites for diffusing species because of energy considerations, one expects to find V enrichment at such boundaries. Experimentally, however, the species which forms at  $\beta$  grain boundaries is Al-rich  $\alpha$  surrounded by V-rich interface.

Evidently the  $\alpha'/\alpha$  interfaces have a more energetically favored position relative to  $\beta$  grain boundaries. Hence, the V moves to these boundaries, leaving the  $\beta$  grain boundaries depleted in V, thereby forming  $\alpha$ .

### Summary

- (1) Microstructure is sensitive to type of quench
- (2) Microstructure is sensitive to solution treatment
- (3) Phases present are not simple  $\alpha$  and  $\beta$
- (4) Producing phases:
  - $\alpha$ : (Type-1  $\alpha$ , Type-2  $\alpha$ , equilibrium, primary acicular, Widmanstätten)
  - $\beta$ : retained, intergranular, enriched, depleted
  - $\alpha'$ : transformed  $\beta$  with same composition as  $\beta$ ; martensite (HCP)
  - $\alpha''$ : Martensite, enriched, depleted
  - $\gamma$ :  $\text{Ti}_3\text{Al}$
  - $\delta$ :  $\text{Ti}_2\text{Al}$
- (5) Allotriomorphs at prior- $\beta$  grain boundaries are  $\alpha$ , but  $\beta$  is present at interfaces.
- (6) Pseudo-binary phase diagrams commonly employed are useful only as trend indicators.
- (7) Ternary diagrams indicate a rich array of phases present.

- (8) Nucleation of  $\alpha$  or  $\beta$  is not well understood.
- (9) Generation of  $\alpha$ " requires further study to define its role in nucleation of  $\alpha$ ,  $\beta$ .
- (10) The importance of  $\gamma$  (or  $\Delta$ ) phase is not well understood.

#### References

1. M. Imam and C. Gilmore, "New Observations of the Transformations in Ti-6Al-4V," in Proceedings of Titanium '80, Vol. 2, Ed. by H. Kimura and O. Izumi (Metallurgical Society of AIME, Warrendale, PA, 1980), p. 1533.
2. Y. Murakami, "Phase Transformation and Heat Treatment," in Proceedings of Titanium '80, Vol. 1, Ed. by H. Kimura and O. Izumi (Metallurgical Society of AIME, Warrendale, PA, 1980), p. 153.
3. J. C. Chesnutt, C. G. Rhodes, and J. C. Williams, "Relationship Between Mechanical Properties, Microstructure, and Fracture Topography in  $\alpha + \beta$  Titanium Alloys," in STP 600 (American Society for Testing and Materials, 1976), p. 1976.
4. J. C. Williams and B. S. Hickman, "Tempering Behavior of Orthorhombic Martensite in Titanium Alloys," Met. Trans. 1, 2648 (1970).
5. M. K. McQuillan, "Phase Transformations in Titanium and its Alloys," Met. Rev. 8(29), 1963.
6. P. J. Fopiano, M. B. Bever, and B. L. Averbach, "Phase Transformations and Strengthening Mechanisms in the Alloy Ti-6Al-4V," Trans. ASM 62, 324 (1969).
7. S. R. Seagle and L. J. Bartlo, "Physical Metallurgy and Metallography of Titanium Alloys," Met. Eng. Q. 8(3), (1968).
8. M. A. ÐYakova, T. G. Potemkina and N. A. Krasilnikova, "Phase Transformation Kinetics in the Alloy VT6," Phys. Met. Metall. 44 (1), 141 (1977).

9. H. Margolin and P. Cohen, "Evolution of the Equiaxed Morphology of Phases in Ti-6Al-4V," in Titanium '80, Vol. 1, Ed. by H. Kimura and O. Izumi (Metallurgical Society of AIME, Warrendale, PA, 1980), p. 1555.
10. C. G. Rhodes and J. C. Williams, "Observations of an Interface Phase in the  $\alpha/\beta$  Boundaries in Titanium Alloys," Met. Trans. A **6A**, 1670 (1975).
11. C. G. Rhodes and N. E. Paton, "The Effect of Heat Treatment on the Nature of the  $\alpha/\beta$  Interface Layer in  $\alpha + \beta$  Titanium Alloys," in Titanium and Titanium Alloys, Eds. J. C. Williams and A. F. Belov (Plenum Press, NY, 1982), p. 1437.
12. G. Welsch, G. Lütjering, K. Gazioglu, and W. Bunk, "Deformation Characteristics of Aged Hardened Ti-6Al-4V," Met. Trans. A **8A**, 169 (1977).
13. P. A. Farrar and H. Margolin, "The Titanium Rich Region of the Titanium-Aluminum-Vanadium System," Trans. Met. Soc. AIME **221**, 1214 (1961).
14. Y. C. Huang, S. Suzuki, H. Kaneko, and T. Sato, "Thermodynamics of the  $M_s$  Points in Titanium Alloys," in The Science, Technology and Application of Titanium Eds. R. I. Jaffee and N. E. Proisel, (Pergamon Press, NY, 1970), p. 691.
15. A. J. Griest, J. R. Daig, and P. D. Frost, "Correlation of Transformation Behavior with Mechanical Properties of Several Titanium-Base Alloys," Trans. Met. Soc. of AIME **215**, 624 (1959).
16. J. C. Williams, "Phase Transformations in Ti Alloys - A Review of Recent Developments," in Titanium and Titanium Alloys, Eds. J. C. Williams and A. F. Belov (Plenum Press, NY, 1982), p. 1437.

17. J. F. Murdock, "Diffusion of Titanium-44 and Vanadium-48 in Titanium," in Diffusion in Body-Centered Cubic Metals (ASM, Metals Park, OH, 1965), p. 262.
18. T. F. Broderick, A. G. Jackson, H. Jones, and F. H. Froes, "The Effect of Cooling Conditions on the Microstructure of Rapidly Solidified Ti-6Al-4V," Met. Trans. A **16A**, 1951 (1985).

## METALLOGRAPHY

In the metallography area, projects in specimen preparation, electropolishing, and powder preparation were carried out. The statistics are summarized below. A patent was filed for preparation of powder using an electro-arc discharge method; this method is described in the abstract for new technology. A number of specimens were electropolished and some of the results reported elsewhere are presented here. An interference method for revealing surface structure was applied and refined, resulting in several presentations on the use of this technique. Interference-layer microscopy has potential for easing many of the problems encountered in examining microstructures of alloys. Instrumentation for carrying out the procedure was obtained and tested. An automated microhardness tester was installed which provides the means of obtaining a statistically acceptable number of indentations for determining the microhardness of specimens, while keeping the amount of time required to a minimum and maintaining excellent reproducibility.

In the paragraphs to follow, summaries of important results not published elsewhere are presented. Tables 10 and 11 contain statistics for the Met and Photo Labs respectively.

Etching problems with powder metal IMI-829 IMPE/AR high-temperature heat-treated parts were encountered; the following procedure was developed to create better contrast between grain boundaries and features in the microstructure.

# IMI 829 P/M ETCHING PROCEDURE

<u>Etchant # 1</u>	15 ml	1. IM reagent
	15 ml	2. Kroll's reagent
	15 ml	H <sub>2</sub> O distilled

- Submerge sample in this solution for 20-30 sec.
- Rinse with sodium bicarbonate and H<sub>2</sub>O.
- Dry with methanol and hot air.

## Etchant # 2

- Submerge sample in Kroll's reagent for 10-15 sec.
- Rinse with sodium bicarbonate and H<sub>2</sub>O.
- Dry sample with methanol and hot air.

NOTE: Etchant # 1 primarily reveals grain boundaries, while Etchant #2 reveals dendritic structure.

1. IM reagent	45 ml	H <sub>3</sub> PO <sub>4</sub>	2. Kroll's reagent	100 ml	H <sub>2</sub> O
	45 ml	H <sub>2</sub> O		4 ml	HNO <sub>3</sub>
	30 ml	HF		2 ml	HF
	15 ml	HNO <sub>3</sub>			

An alloy subjected to this etching procedure is shown in Fig. 8.

TABLE 10  
SUMMARY OF MET LAB STATISTICS

	<u>Number of Specimens</u>
Misc. metals	6
Nonmetals	88
Ti-base alloys	1,804
Al-base alloys	1,095
Ni-base alloys	547
Mg-base alloys	236
Misc. base alloys	255
Electropolished samples	496
Microphotographs	606

TABLE 11  
SUMMARY OF PHOTO LAB STATISTICS

	<u>Number Processed</u>
Contacts	23,447
Enlargements	4,384
Viewgraphs	618
Slides	2,764
Negatives	733
Portraits	53
Color Prints	88

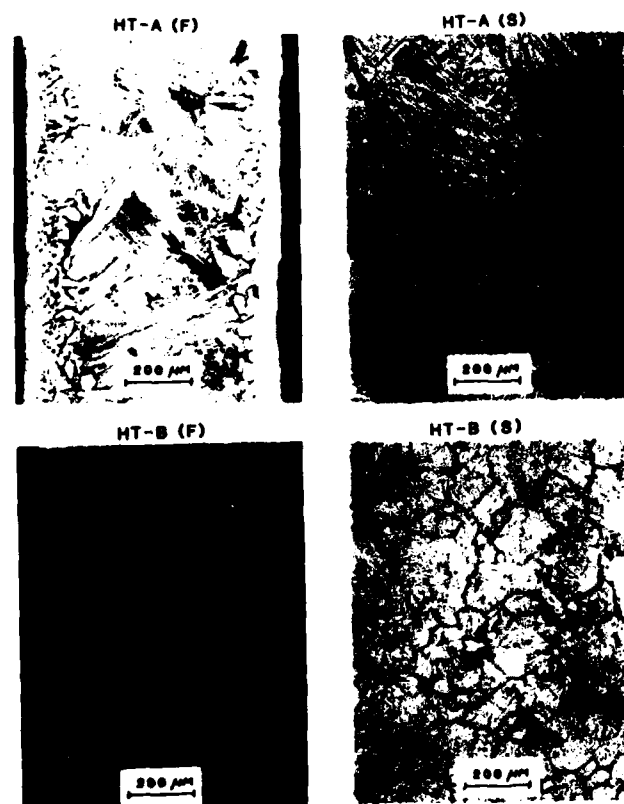


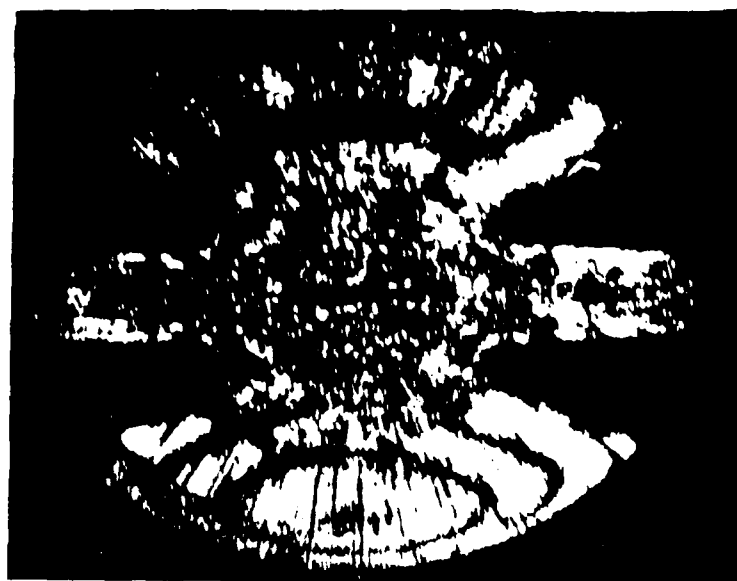
Figure 8. IMI 829 Etched with New Procedure HT-A (F) or Part of Fin, HT-A (S) or Part of Shaft. HT-B (F) and HT-B (S) are same alloy heat-treated at higher temperature.

#### Procedure for Polishing Ends of 3/4 x 3 x 7-in. Plexiglas Fatigue Specimens

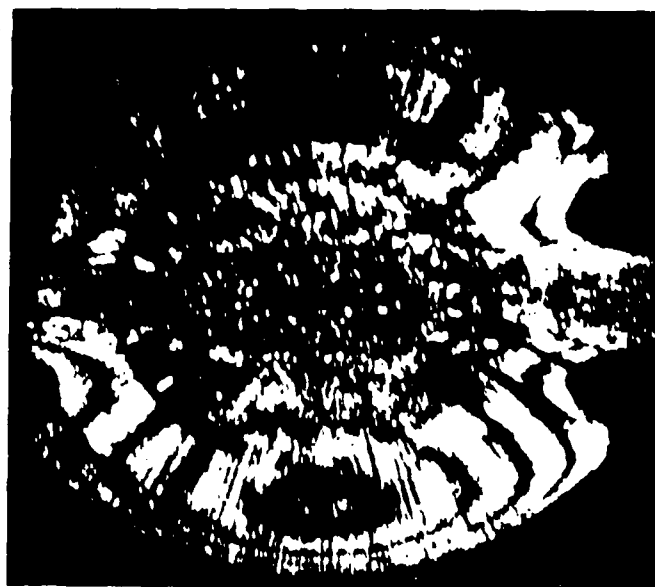
1. When working with Plexiglas sample, check to see which end has least deformation from previous saw cut. Grind that end with 8-in. polisher at 350 RPM with 8-in. PSA 600-grit SiC disc until all deformation is eliminated.
2. Wash in soap and warm water; flush with methanol; blow dry with hot air.
3. Polish on 8-in. polisher with 8-in. PSA nylon cloth, using 3- $\mu$  diamond paste and oil lubricant. Polish at 350 RPM until deformation of 600-grit is completely removed.
4. Clean as in Step #2.
5. Polish on 8-in. polisher with 8-in. PSA microcloth using 0.06- $\mu$  colloidal silicon suspension at 200 RPM until surface is featureless.
6. Clean as in Step #2.

A procedure for polishing the ends of Plexiglas fatigue specimens prior to laser interferometry was developed. This procedure renders the Plexiglas free of optical distortion and allows fracture fringes to be photographed through the ends of the specimens. Figure 9(a) - 9(c) show the results of this polishing technique.

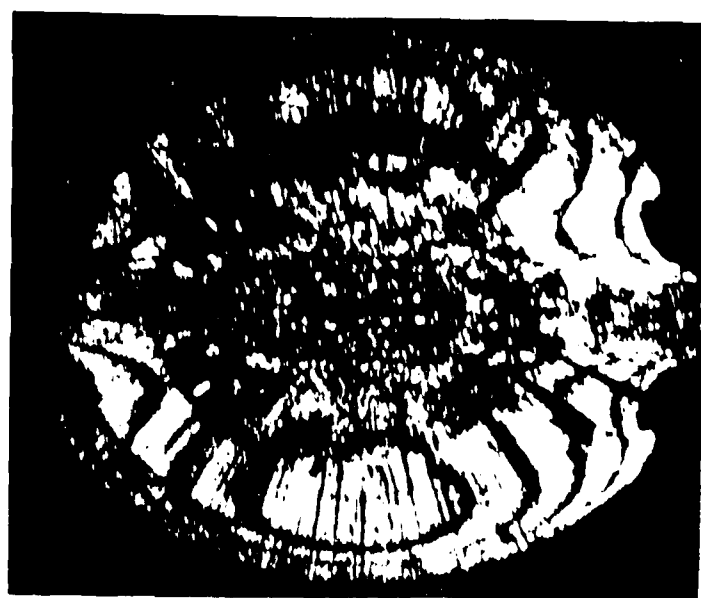




(a)



(b)



(c)

Figure 9. Flexiglas under (a) Low Load, (b) Medium Load, and (c) High Load.

## Electrolytic Polishing Techniques for RST Ti Alloy Ribbons

Several problems associated with metallographic preparation of Ti-alloy ribbons have caused metallographers to search for new ways to prepare this material. Because of the size, shape, and inhomogeneities of samples, some ribbons cannot be prepared by mechanical methods. Previously encountered problems include retaining the edge, working the surface of the sample, and retaining small features in the structure, such as alloyed precipitates. Also because of the sample size, it was thought to be impossible to shape this material by electrochemical polishing. Several attempts to use techniques for mounting the ribbons failed because of rounding of the edges and uneven currents which cause furrowing in the sample. A new sample conductive mounting medium (Konductomet I) was recently purchased from Buehler, Ltd. With this carbon-filled phenolic compound, uniform contact with all samples was made, reducing the resistivity and producing a more stable polish. The use of electro-polish/etch procedures along with Konductomet I has eliminated three problems previously encountered with mechanical polishing/chemical etching (see Figs. 10 and 11):

1. Smearing of the surface,
2. Introduction of chemical artifacts onto the surface, and
3. Polishing/etching difficulties associated with ribbons.



Figure 10. Scanning Electron Micrograph of Electropolished Ti-9Co Showing Improved Detail of Grain Boundaries and Edge Retention at 400x.



Figure 11. Scanning Electron Micrograph of Electropolished Ti-9Co Showing Greatly Improved Definition of Coarse- $\alpha$  Precipitation from Grain Boundaries in Matrix of Fine  $\alpha$ .

Mechanical polishing introduces surface deformation and edge rounding which results in an overall haze on the surface when etched. Resolution of the surface--both optically and through the use of electron optics--is difficult (see Figs. 12 and 13).



Figure 12. Scanning Electron Micrograph of Mechanically Polished Ti-9Co Surface at 200x; Entire Surface is Rounded and Pitted.



Figure 13. Scanning Electron Micrograph of Mechanically Polished Ti-9Co; High-Magnification Resolution of Basket-Weave  $\alpha$ .

The polishing curve for Ti-9Co was developed at  $-30^{\circ}\text{C}$  (see Fig. 14). Polishing occurred in a wide range from 7 to 36 V, and etching occurred between 11 and 14 V--a very small range and very difficult to control. By reducing the temperature of the electrolyte to  $-45^{\circ}\text{C}$ , the polishing and etching ranges are extended, making it easier to control the process (see Fig. 15).

Research on the new interference-layer technique was conducted. Some success was achieved with the aluminum-alloyed button melts, but the techniques for final polishing of the sample must be perfected. An invited paper on the technique was presented at the ASM Conference in Orlando, FL, October 3-6, 1986.

Twenty successful runs were made in the recently modified EDM which is used for spark erosion of metals in a cryogenic dielectric. Seven Ti-alloyed extrusion rods were sectioned into electrodes and spark eroded in liquid nitrogen. Sample K-4 Ti4W (Fig. 16) exhibits no elemental change, but the structure of the powder (Fig. 17) shows that the process has affected the microstructure. Aluminum alloys and amorphous metals were spark eroded in liquid nitrogen.

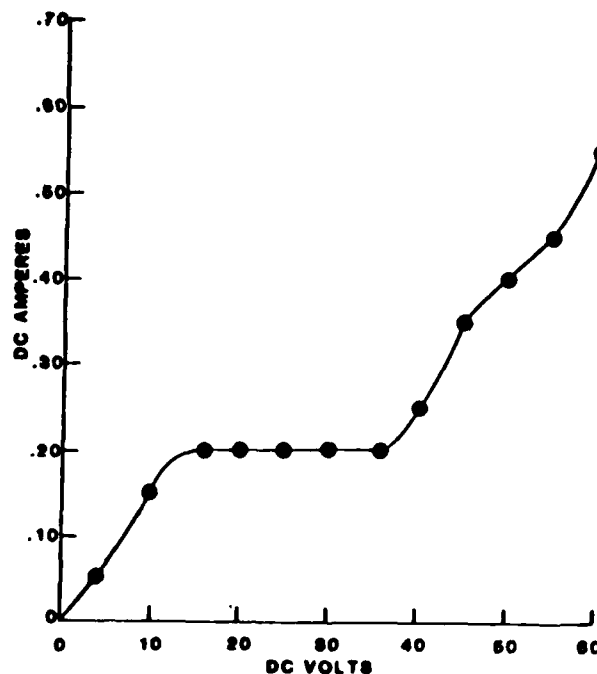


Figure 14. Current-Voltage Curve for K-18 Series Ti-9Co  
(3 Min., 9-mm Developed at Diameter,  $-30^{\circ}\text{C}$ .)

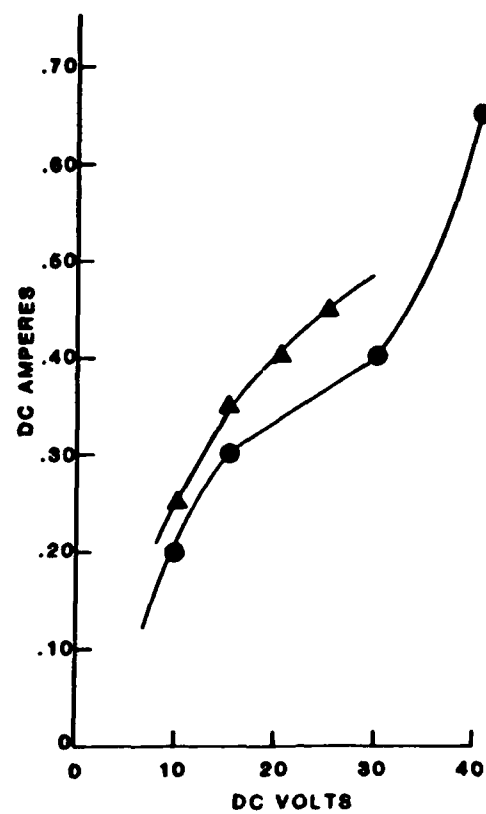


Figure 15. Current-Voltage Curve for K-18 Series Ti-9Co (60 Min. at  $-45^{\circ}\text{C}$ ).



Figure 16. Energy-Dispersive Spectrum of Ti-4W.

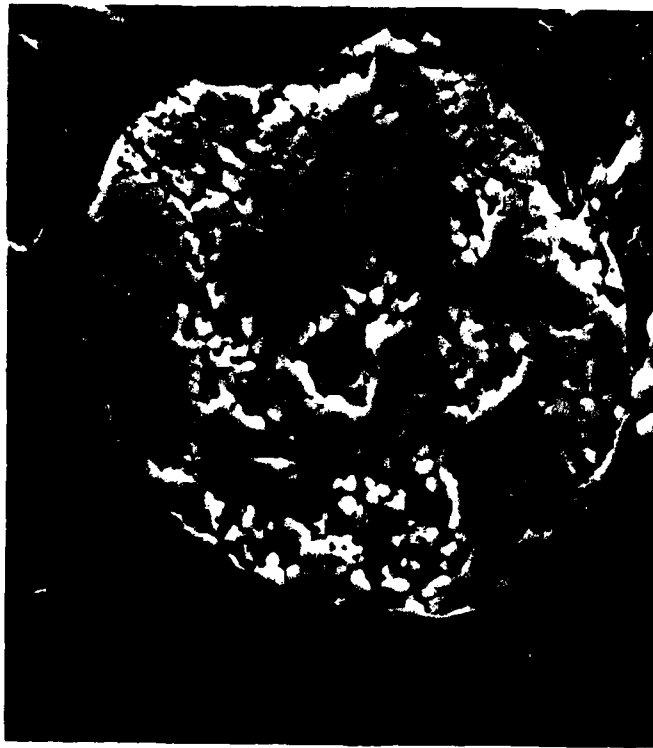


Figure 17. Scanning Electron Micrograph of Ti-4W Rod Spark Eroded in Liquid Nitrogen. (2000x)

#### Electropolishing vs Mechanical Polishing

According to the literature on electropolishing in Metals Handbook, Vol. 9, "Artifacts resulting from mechanical deformation, such as distributed metal or mechanical twins which are produced on the surface even by careful grinding and mechanical polishing ... do not occur in electropolishing ... surfaces are completely unworked by the polishing procedure, which is particularly beneficial in low load hardness testing."

Since efforts in the lab consist of frequent low-load hardness testing, a simple experiment was employed. A Ti-6Al-4V rod was sectioned, mounted in Epomet, and prepared to a final polish using an etch/polish technique four to five times in the final polishing sequence. A scribe line (Fig. 18) was drawn in the middle of the sample to landmark the hardness testing. Knoop hardness tests at 2, 5, 10, 25, and 50 gm were implemented with approximately 10 indentations per test (Fig. 18). The semi-automatic hardness was

set up in the trace mode; hardness test variables such as distance between indents, load, dwell time, and direction were controlled. Indents were made automatically, while readings were made manually. After the five tests had been made on the mechanically polished sample, it was electro-polished in 60 ml perchloric acid, 60% 350 ml butyl cellosolve, and 590 ml methanol under conditions of medium agitation at  $-53^{\circ}\text{C}$ , 2.0 A for 5 min. The sample was then washed and dried and the same five Knoop hardness tests executed in the manner described above (see Fig. 19). Table 12 contains the results.



Figure 18. Mechanically Polished Ti-6Al-4V Rod after 50-gm Knoop Hardness Testing (133x).





Figure 19. Electropolished Ti-6Al-4V Rod after 50-gm Knoop Hardness Testing (133x).

#### SRL/R.A.R.E. SYSTEM

Electropolishing, when properly applied, can be a useful metallographic specimen-preparation technique. For some metals, electropolishing can produce a high quality finish that is equal to or better than the best surface finish obtainable by mechanical polishing methods. Specimens prepared by electropolishing exhibit surfaces free of artifacts resulting from mechanical deformations. Also since the surfaces are completely unworked by the polishing procedure, electropolished specimens are ideal for low-load hardness testing, X-ray studies, and electron microscopy.

Electropolishing has certain disadvantages. Mainly, a different set of conditions and electrolytes is required to obtain a satisfactorily polished surface for each alloy. Consequently, considerable time may be required to develop the polishing parameters which produce the desired surface finish.

Table 12  
COMPARISON OF TESTS PERFORMED ON MECHANICALLY POLISHED  
AND ELECTROPOLISHED SPECIMENS

	Mechanically Polished Ti-6Al-4V Rod	Electropolished Ti-6Al-4V Rod
<b>Test #1</b>	<b>2 gm KNH</b>	<b>2 gm KNH</b>
indents	9	9
mean	261.4	266.95
standard deviation	31.84	43.42
high	308.8	351.3
low	231.0	215.1
<b>Test #2</b>	<b>5 gm KNH</b>	<b>5 gm KNH</b>
indents	10	10
mean	322.26	328.43
standard deviation	29.21	31.59
high	363.0	368.20
low	277.9	312.0
<b>Test #3</b>	<b>10 gm KNH</b>	<b>10 gm KNH</b>
indents	10	10
mean	350.99	354.26
standard deviation	21.23	34.76
high	382.0	394.1
low	310.7	294.0
<b>Test #4</b>	<b>25 gm KNH</b>	<b>25 gm KNH</b>
indents	11	10
mean	327.96	326.18
standard deviation	13.21	21.40
high	349.4	363.1
low	307.7	297.2
<b>Test #5</b>	<b>50 gm KNH</b>	<b>50 gm KNH</b>
indents	20	9
mean	326.99	319.54
standard deviation	12.62	9.11
high	349.8	331.8
low	311.4	302.5

In the Materials Characterization Facility new and unusual alloys are analyzed. Due to the uniqueness of these materials, appropriate electropolishing procedures have not been developed. As mentioned above, this is a time-consuming process. In order to take advantage of the benefits of electropolishing in this laboratory situation, a tool capable of generating appropriate electropolishing parameters in a timely fashion was developed. This tool is discussed below.

The SRL/R.A.R.E. System is a computer-controlled electropolisher designed to generate the characteristic electropolishing curve for a given set of conditions. This characteristic curve reveals to the metallographer a range of cell potentials and current densities which will produce the desired surface finish for a given specimen, electrolyte, cell temperature, stirring set-point, and cell geometry. The system can generate a characteristic curve in  $\sim 10$  min. This task previously required about 8 hr of tedious labor using traditional techniques. Thus, by varying one parameter at a time, a family of curves can be generated which illustrates the effect of each parameter on the characteristic electropolishing curve. More importantly, an operator interested only in polishing a specimen can typically do so with the data obtained from one curve. This means that the operator can generate the data required to electropolish a particular specimen and polish that specimen to a suitable surface finish in  $\sim 30$  min. This three-cell electropolishing system is capable of performing an electropolishing experiment under computer control, while two other specimens are being electropolished manually.

The operator-to-system interface is achieved through menu-driven software specifically designed to be user friendly at all levels of operation. Computer programming skills are not required to operate the system. Five main programs are available to the operator from the system main menu. These five programs allow the operator to become familiar with the system and its capabilities, access the material and electrolyte libraries, add to or change entries in these libraries, perform an electropolishing experiment under computer control, and recall data from the system data base for analysis, comparison, and graphic presentation. A brief description of each of the five main system programs is given below.

The system-description program (Option A on the system main menu) provides the operator with a description of the system capabilities and the components which comprise the system. This program highlights the specifications of the individual components and explains their role in the overall operation of the system. The operator can either page through the program by using the function keys on the keyboard or, by pressing one key, output the entire system description to the printer and obtain a hard copy.

The electrolyte and material library program (Option B on the system main menu) serves several purposes. It provides a list of recommended electrolytes for polishing various metal alloys. It also provides access to an extensive list of electrolytes, their chemical compositions, and the safety precautions regarding their use. By choosing the appropriate menu option, the operator can view the information on the CRT or obtain a hard copy of the information from the printer. In addition, this program provides access to the material library for viewing on the CRT or in hard-copy form.

The electropolishing experiment program (Option C on the system main menu) generates the characteristic electropolishing curve for a given set of conditions. The program prompts the operator to enter the parameters such as cell temperature, voltage increment, stirring set point, and temperature tolerance. The system then automatically generates the characteristic electropolishing curve while displaying the results in real-time on the CRT. All parameters are controlled and monitored automatically, allowing the operator to analyze the data while it is being generated. A hard copy of the data is produced during the experiment to prevent loss of data in case of a catastrophic system failure. Upon completion of the experiment, the operator has the option of writing the data to a file in the system data base. If this option is exercised, the data, including all pertinent experimental parameters, are stored on the hard disk for future retrieval.

The data base/analysis program (Option D on the system main menu) permits access to data stored in the system data base. This program provides the capability for preferential and sequential search of the existing data files with respect to work order number, initiating engineer, electrolyte composition, and material composition. This allows the operator to analyze a

particular file or group of files of interest. The data base can hold 10,000 files on line and an unlimited number on diskette. Another feature of the data base/analysis program is the ability to output the results of an experiment in graphic form. Data from up to three files can be plotted on the same graph for comparison purposes. These graphs can be output to the CRT or to the six-pen color plotter.

The library edit program (Option E on the system main menu) allows the operator to add, delete, or change entries in the electrolyte and material library files.

Since the SRL/R.A.R.E. System is software based, it can evolve to satisfy the changing needs of the research environment for which it was designed. The system controller, an IBM PC-AT, was chosen to offer the highest degree of compatability with existing and future laboratory equipment.

#### Results Obtained Using the SRL/R.A.R.E. System

Some results obtained using the SRL/R.A.R.E. System are illustrated in the graphs on the following pages. The data were recalled from the system data base and plotted using the data-base analysis program. Figure 20 shows the current-vs-voltage relationship for a Ti-6Al-2Sn-4Zr-6Mo specimen (Material Code 1-2) polished in an electrolyte composed of 590 ml methanol, 350 ml butyl-cello-solve, and 60 ml of 60% perchloric acid (Electrolyte Code 1-11). The parameter of interest is the electrolyte temperature (-65°C). The general shape of the curve conforms to the stereotypical curve obtained when using this electrolyte.\* The polishing region is observed to lie between cell potentials of 13 and 23 V, resulting in an anodic current of  $\sim 0.14$  A. Figure 21 gives the results obtained for an electrolyte temperature of -60°C; all other parameters remain the same. The polishing region in this case is observed to lie between cell potentials of 12 and 18 V, resulting in an anodic current of  $\sim 0.15$  A. Figure 22 illustrates the effect of varying the electrolyte temperature 5°C by plotting both sets of data on the same graph.

---

\*Metals Handbook, 9th Edition, Vol. 9.

One can theorize from these results that electrolyte temperature is a critical parameter of electropolishing. Further experiments currently being conducted to document the effect which electrolyte temperature has on the polishing region reinforce the above mentioned theory.

### Summary

Electropolishing can be a very useful metallographic specimen-preparation technique. The major drawback is the tedious and time-consuming task of developing procedures for electropolishing new metal alloys. The AFWAL Materials Laboratory Materials Characterization Facility is interested mainly in metal alloys for which electropolishing procedures have not been established. To realize the benefits of electropolishing in such a laboratory environment, a tool for generating electropolishing procedures for new alloys in a timely manner was developed for the metallographer. This system, the SRL/R.A.R.E. System, generates characteristic electropolishing curves and stores the data for future analysis, comparison, and graphic output. The system is software based and, thus, can evolve to meet the changing needs of the laboratory.

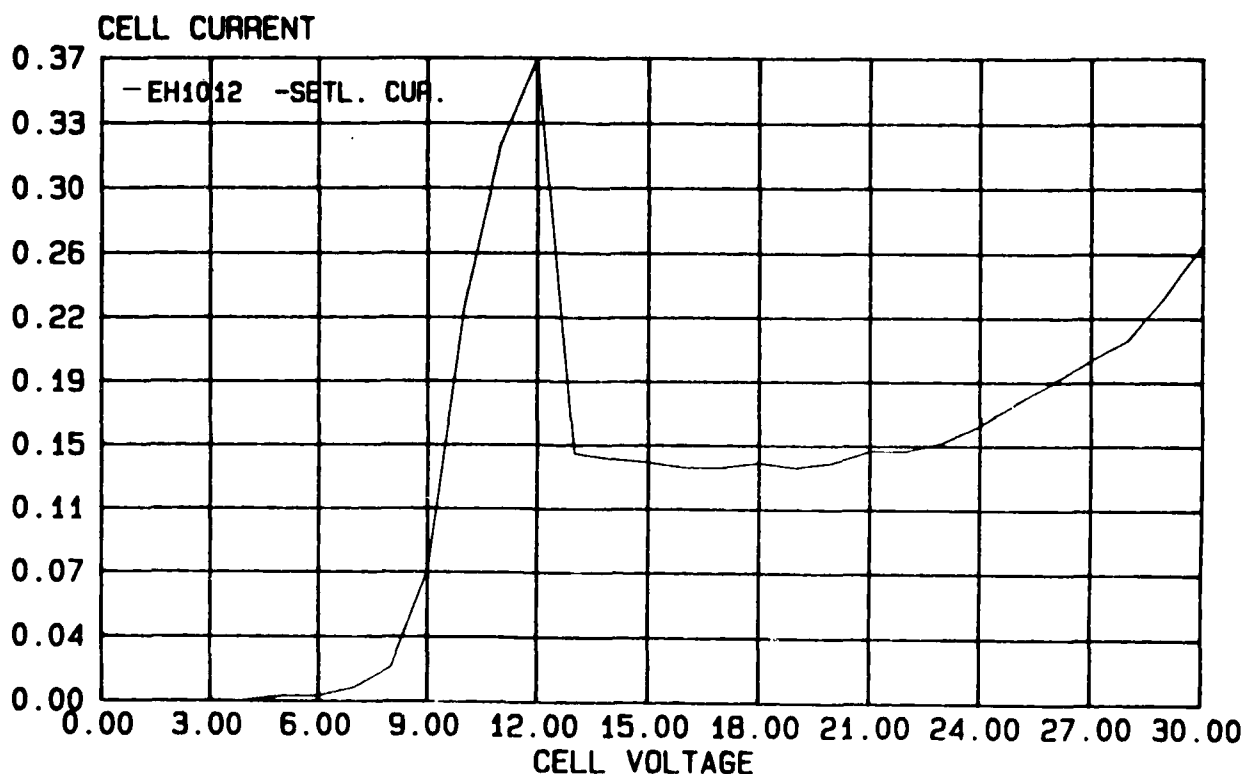


Figure 20. Graph Showing Current-vs-Voltage Relationship for Ti-6Al-2Sn-4Zr-6Mo Specimen.

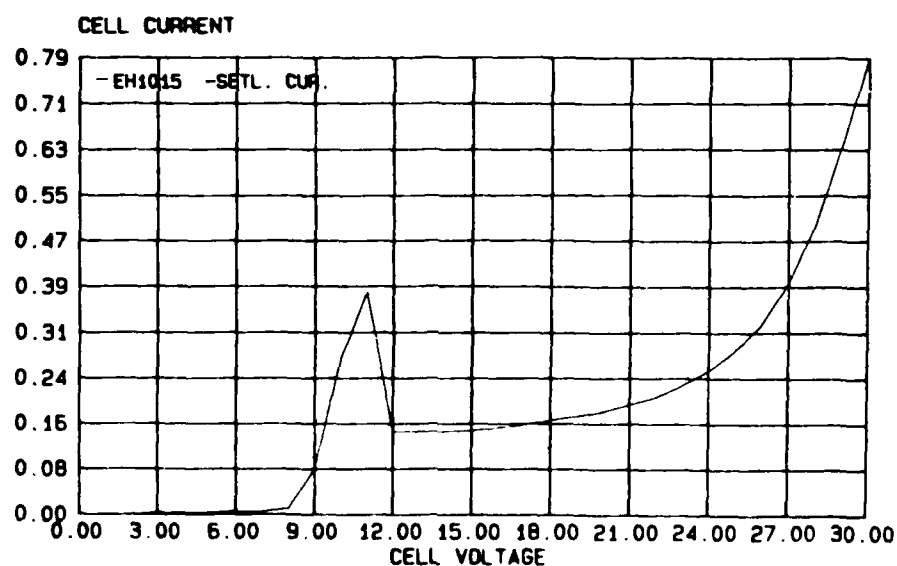


Figure 21. Curve Depicting Results Obtained for Electrolyte Temperature of  $-60^{\circ}\text{C}$  for Ti-6Al-2Sn-4Zr-6Mo Specimen.

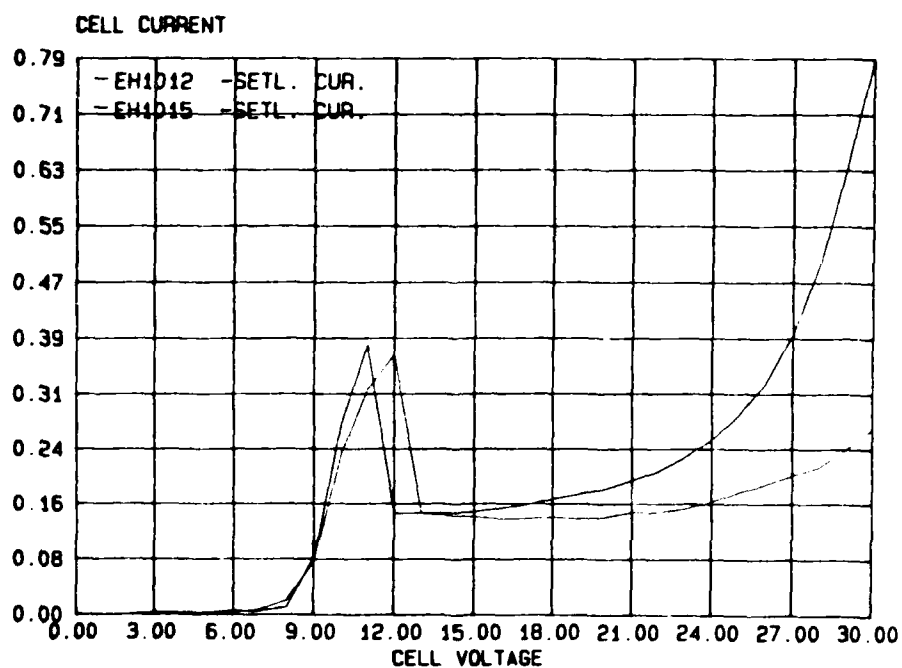


Figure 22. Graph Illustrating Effect of Varying Electrolyte Temperature  $5^{\circ}\text{C}$  by Plotting both Sets of Data on Same Graph.

## RAPID-SOLIDIFICATION EQUIPMENT

A large portion of the research conducted on this program was concerned with detailed characterization of microstructures present in rapidly solidified (RS) alloys, particularly Ti-, Al- and Mg-base alloys. Difficulties in obtaining material were experienced early in the program; to remedy this situation several rapid-solidification instruments were designed and constructed. Having such equipment available significantly improved the pace of the research and provided the means for identifying and controlling the quality of the product under study.

Three types of RS instruments were constructed--pendant drop melt extraction, melt spin (also known as chill block), and splat quench. The pendant drop melt extraction system consists of a rotating disk made of copper, steel, or titanium which is oriented in such a way that a rod can be held above the edge of the disk. The rod is melted using an electron emitter (W filament) biased at several thousand volts and capable of producing up to 3 kw of power. As the tip of the rod becomes liquid, the rod is lowered until the liquid ball at the tip touches the rotating disk, causing the liquid to be pulled off the ball onto the disk and solidify into a ribbon of alloy. The system operates in a vacuum of  $10^{-6}$  Torr or better. Most of the Ti alloys characterized were produced using this approach.

The melt spin system is of similar design with respect to the rotating disk, but the rod is replaced by a crucible in which the alloy is placed. Melting takes place by means of an RF heater capable of producing up to 60 kw of power. Upon melting, the liquid alloy is forced from the crucible through an orifice in the bottom by applying a positive inert-gas pressure through the top of the crucible. Ribbons up to 25.4 mm in width have been produced using the melt spinner. The system operates at atmospheric pressure but is capable of being shrouded if inert-gas atmosphere is desired. This system found application in the production of Al and Mg alloys primarily.

For splat quenching of alloys, a design based on that in use at the University of Sheffield, UK, was constructed. In this method, a small quantity of alloy is melted and levitated by an RF heater. When the alloy



is liquid, the heater is turned off and the alloy drops through an optical sensor which triggers two opposing disks driven by a high gas pressure. The passage of the alloy drop through the sensor and to the hammers is timed by a trigger circuit in order that the alloy drop will be at the center of the two hammer heads when the hammers are slammed together to produce the splat material. Alloys of Mg and Ti have been produced using this system. It is located in a closed glove box to allow for positive control of the atmosphere and to keep oxygen levels at the absolute minimum, which is especially important for Mg alloys.

### Section 3

#### PAPERS, PRESENTATIONS, EXHIBITS, AND INVENTIONS

The characterization research efforts conducted during this contract resulted in the publication of 9 papers, presentation of 16 papers which were subsequently published in conference proceedings, presentation of 6 papers which were not published, and presentation of 6 posters. Multiple authorship with AFWAL Materials Laboratory and other contractor personnel was common since the research encompassed a wide range of study. In addition, a number of photographic exhibits were submitted to the International Metallographic Society for competition in format and content presentation. A number of the exhibits were declared winners in their categories.

#### PAPERS AND PRESENTATIONS

"Beta Eutectoid Decomposition in RS Titanium-Nickel Alloys," A. G. Jackson, S. Krishnamurthy, F. H. Froes, and H. Jones, In preparation for Met. Trans.

"Prediction of Holz Pattern Shifts in Convergent-Beam Diffraction," A. G. Jackson, Accepted for publication in J. Electron Microscopy Technique, 1986.

"Identification of  $Al_{20}Ti_2Gd$  Precipitates in an Aged RST Al-4Ti-4Gd Alloy," A. G. Jackson, Y. R. Mahajan, and S. D. Kirchoff, Scripta Metal. 20(9), 1247 (1986).

"Phases and Orientation Relationships in a Rapidly Solidified Al-6Fe-6Ni Alloy," Y-W Kim and A. G. Jackson, Scripta Metal. 20, 777 (1986).

"The Ultrastructural Localization of Tri-N-Butylin in Human Erythrocyte Membranes during Shape Transformation Leading to Hemolysis," M. Porvazuik, B. Gray, D. Mattie, A. G. Jackson, and R. E. Omlor, Lab. Investigation 34, 254 (1986).

"An Electron Microscope Study of the Morphology of Cured Epoxy Resin," R. E. Omlor, V. B. Gupta, L. T. Drzal, and W. W. Adams, J. Mater. Sci. 20, 3439 (1985).

"Analytical Microscopy of Precipitates in Rapidly Solidified Alloys," A. G. Jackson, J. Metals 37, 46 (February 1985).

The Effect of Cooling Conditions on the Microstructure of Rapidly Solidified Ti-6Al-4V," A. G. Jackson, T. F. Broderick, and F. H. Froes, Met. Trans. 16A (1985).

"On the Effect of NaCl on Porosity in Elemental-Blend Powder Metallurgy Ti-5Al-2.5Sn," A. G. Jackson, J. Moteff, and F. H. Froes, Met. Trans. 15A, 2118 (January 1984).

"Rapidly Solidified  $Ti_3Al$ ," C. H. Ward, K. R. Teal, A. G. Jackson, and F. H. Froes, Presented at the ASM Symposium, Lake Buena Vista, FL, 4-9 October 1986; to be published in the conference proceedings.

"Evaluation of the Effects of PDME Operating Parameters on the Reproducibility of Titanium Ribbon Product," P. R. Smith, J. G. Paine, and S. Krishnamurthy, Presented at the ASM Symposium, Lake Buena Vista, FL, 4-9 October 1986; to be published in the conference proceedings.

"Aging Response of Rapidly Solidified Titanium-Tungsten Alloy with Nickel and Silicon Additions," S. Krishnamurthy, A. G. Jackson, I. Weiss, and F. H. Froes, Presented at the ASM RS Conference, San Diego, CA, 3-5 February 1986; published in the conference proceedings.

"Aging Response of Rapidly Solidified Titanium-Tungsten Alloys," D. Eylon, I. Weiss, F. H. Froes, A. G. Jackson, and S. Krishnamurthy, Presented at the Third Israel Materials Engineering Conference, Haifa, Israel, December 1985, and published in Titanium-Rapid Solidification Technology, edited by F. H. Froes, D. Eylon, and S. M. L. Sastry (TMS Publications, Warrendale, PA, 1986).

"The Morphology of Cured Epoxy Resin," L. T. Drzal, W. W. Adams, V. B. Gupta, P. F. Lloyd, and R. E. Omlor, Exhibited at the Annual Meeting of the Electron Microscopy Society of America, Detroit, MI, 13-20 August 1986.

"Microstructure of Rapidly Solidified  $Ti_3Al$  Alloys," A. G. Jackson, K. R. Teal, D. Eylon, F. H. Froes, and S. Savage, Presented at the Materials Research Society 1985 Fall Meeting, Symposium J, Boston, MA, 2-4 December 1985, and published in Rapidly Solidified Alloys and Their Mechanical and Magnetic Properties, Vol. 58, edited by B. C. Giessen, D. E. Polk and A. I. Taub (Materials Research Society, Pittsburgh, PA, 1986), p. 365.

"Small Angle Electron Scattering (SAES) of Polymers," S. Kumar, W. W. Adams, P. F. Lloyd, and R. E. Omlor, Presented at the Joint Meeting of the Electron Microscopy Society of America and the Microbeam Analysis Society, Louisville, KY, 5-10 August 1985; abstract published in the conference proceedings.

"Investigation of a Rapidly Solidified Al-Lanthanide Alloy," A. G. Jackson, S. J. Savage and F. H. Froes, Presented at the Fifth Int. Conf. on Titanium, Munich, West Germany, 10-14 September 1984; published in the conference proceedings.

"Rapidly Solidified Microstructures of Titanium Alloys Containing Eutectoid Forming Additions," A. G. Jackson, S. Krishnamurthy, D. Eylon, B. Boyer and F. H. Froes, Presented at the Fifth Int. Conf. on Titanium, Munich, West Germany, 10-14 September 1984; published in the conference proceedings.

"Microstructures of Rapidly Solidified Ti-5Al-2.5Sn with Si or Ge Additions," A. G. Jackson, T. F. Broderick and F. H. Froes, Presented at the Fifth Int. Conf. on Titanium, Munich, West Germany, 10-14 September 1984; published in the conference proceedings.

"Microstructures and Properties of a Rapidly Solidified Aluminum-Gadolinium Alloy," A. G. Jackson, S. J. Savage, Y. R. Mahajan, and F. H. Froes, Presented at the Fifth International Conference on Rapidly Quenched Metals, Wurzburg, West Germany, 3-7 September 1984; published in the conference proceedings.

"Rapidly Solidified Microstructures and Precipitation in a Ti-5.5 w/o Ni Alloy," A. G. Jackson, S. Krishnamurthy, D. Eylon, R. R. Boyer, and F. H. Froes, Presented at the Fifth Int. Conf. on Rapidly Quenched Metals, Wurzburg, West Germany, 3-7 September 1984; published in the conference proceedings.

"Cooling Rate Effects on Ti-6Al-4V and Beta III Titanium Alloys," A. G. Jackson, T. F. Broderick, and F. H. Froes, Presented at MRS Symposium on Rapidly Solidified Metastable Materials, Boston, MA, 14-17 November 1983; published in the conference proceedings.

"Mark II Test Vehicle Holder for In-Situ Viewing of Integrated Circuit Electromigration," J. V. Maskowitz, W. E. Rhoden, D. R. Kitchen, R. E. Omlor, and P. F. Lloyd, Presented at the Joint Meeting of the Electron Microscopy Society of America and the Microbeam Analysis Society, Albuquerque, NM, 10-15 August 1986; published in the conference proceedings.

"preparation of Integrated Circuits for TEM Electromigration In-Situ Studies," J. V. Maskowitz, W. E. Rhoden, D. R. Kitchen, R. E. Omlor, and P. F. Lloyd, Presented at the Joint Meeting of Electron Microscopy Society of America and the Microbeam Analysis Society, Albuquerque, NM, 10-15 August 1986; published in the conference proceedings,.

"In-Situ STEM Observation of Electromigration on Thin Aluminum Strips," J. V. Maskowitz, W. E. Rhoden, D. R. Kitchen, R. E. Omlor, and P. F. Lloyd, Presented at the Joint Meeting of the Electron Microscopy Society of America and the Microbeam Analysis Society, Albuquerque, NM, 10-15 August 1986; published in the conference proceedings.

"Rapid Solidification of Aluminum-Lanthanide Alloys," A. Jackson, S. J. Savage, Y. R. Mahajan, and F. H. Froes, Presented at The Metals Society Fall Meeting, Detroit, MI, 17-20 September 1984.

"Fundamental Studies of the Microstructure of Rapidly Solidified  $Ti_3Al$  and  $Ti_3Al-Nb$ ," K. R. Teal, A. G. Jackson, D. Eylon, and F. H. Froes, Presented at the 115th TMS Annual Meeting, New Orleans, LA, 2-6 March 1986.

"Thermal Stability of RST Al-Ti-Gd Alloy," V. Mahajan, S. Kirchoff and A. G. Jackson, Presented at the 115th TMS Annual Meeting, New Orleans, LA, 2-6 March 1986.

"Rapid Solidification of Titanium-Eutectoid Former Alloys," S. Krishnamurthy, I. Weiss, A. G. Jackson, D. Eylon, and F. Froes, Presented at the 115th TMS Annual Meeting, New Orleans, LA, 2-6 March 1986.

"Preparation of Award Winning Microstructures," E. Harper, An invited presentation at the Central Ohio Metallographic Society Meeting, Columbus, OH, 16 October 1986.

"Microstructure of Rapidly Solidified Al-5.8Fe-6.1 Ni Alloy Powder," A. G. Jackson and Y-W. Kim, Presented at the Metallurgical Society of AIME Meeting, Toronto, Canada, 14-15 October 1986.

"Rapid Solidification Technology of Ti," A. G. Jackson, Invited Presentation at the Columbus, Ohio, Section of the Central Ohio Metallographic Society, Columbus, OH, 14 March 1984.

"Rapid Solidification Technology of Ti," A. Jackson, Invited Presentation at the Dayton Chapter of ASM, Dayton, OH, 8 February 1984.

"The Relationship Between Cooling Rate and Grain Size in RST Ti-6Al-4V," A. Jackson, T. F. Broderick and F. H. Froes, Presented at the Metallurgical Society of AIME Meeting, Los Angeles, CA, 27 February 1984.

"Analysis of Subprecipitates in  $Ti_5Si_3$  in Aged Ti-5Al-2.5Sn-5Si," A. G. Jackson, F. H. Froes, and J. Moteff, Presented at the TMS-AIME Fall 1983 Meeting, Philadelphia, PA, October 1983.

"A BASIC Program for Calculating Zones and Planes in TEM Electron Diffraction Patterns," A. G. Jackson, Presented at the TMS-AIME Fall 1983 Meeting, Philadelphia, PA, October 1983.

"Mechanical Properties and Corrosion Behavior of Rapidly Solidified Mg-Ca-Cu and Mg-Ca-Ni Alloys," A. G. Jackson, F. Hehmann, S. Krishnamurthy, E. Robertson and S. Savage, Presented at the International Powder Metallurgy Conference 1986, Dusseldorf, West Germany, 7-11 July 1986; published in the conference proceedings.

## EXHIBITS

"My Dog Nitride," R. D. Brodecki, Exhibited at the International Metallographic Society 19th Annual Convention, Boston, MA, 2-6 August 1986. Received honorable mention in Class 7. Part of a traveling international exhibit.

"A Snails Pace," R. D. Brodecki, Exhibited at the International Metallographic Society 19th Annual Convention, Boston, MA, 2-6 August 1986. Part of a traveling international exhibit.

"Low Density Ti-Zr-Be Alloy," H. Bomberger, C. Cooke, M. Dodd, and R. D. Brodecki, Exhibited at the International Metallographic Society 19th Annual Convention, Boston, MA, 2-6 August 1986. Part of a traveling international exhibit.

"Heat Wave," J. C. Heidenreich, Exhibited at the International Metallographic Society 19th Annual Convention, Boston, MA, 2-6 August 1986. Part of a traveling international exhibit.

"Water Lilies," S. D. Apt, P. F. Lloyd, and R. E. Omlor, Exhibited at the International Metallographic Society 19th Annual Convention, Boston, MA, 2-6 August 1986. Part of a traveling international exhibit.

"Rapid Solidification Technology," P. F. Lloyd, R. E. Omlor, S. D. Apt and J. G. Paine, Exhibited at the International Metallographic Society 19th Annual Convention, Boston, MA, 2-6 August 1986. Part of a traveling international exhibit.

"'Bobby' Pin Technique," J. S. Hennessee and R. K. Lewis, Exhibited at the International Metallographic Society 19th Annual Convention, Boston, MA, 2-6 August 1986. Part of a traveling international exhibit.

"Molybdic Acid Vs Kroll's as Ti Etchant," R. K. Lewis and V. L. Weddington, Exhibited at the International Metallographic Society 19th Annual Convention, Boston, MA, 2-6 August 1986. Part of a traveling international exhibit.

"Frozen Microstructures," E. Harper, R. J. Bacon, F. O. Deutscher, S. J. Savage, and I. Weiss, Exhibited at the 18th Annual International Metallographic Society Meeting, Denver, CO, 21-24 July 1985. Received Second Place in Class 6 - Electron Microscopy - Scanning. Part of a traveling international exhibit.

"Interferenzschichten - Mikroskopie," E. Harper and Y. M. Mahajan, Exhibited at the 18th Annual International Metallographic Society Meeting, Denver, Co, 21-24 July 1985. Received Second Place in Class 9 - Color Micrographs From any Class. Part of a traveling international exhibit.

"Tropical Dream," E. Harper and J. G. Paine, Exhibited at the 18th Annual International Metallographic Society Meeting, Denver, CO, 21-24 July 1985. Received Third Place in Class 7a - Pretty Microstructures - Color Only. Part of a traveling international exhibit.

"Dendroid," R. J. Bacon, C. R. Underwood, and S. J. Savage, Exhibited at the International Metallographic Society 18th Annual Meeting, Denver, CO, 21-24 July 1985. Part of a traveling international exhibit.

"Stormy Weather," R. Brodecki and M. Dodd, Exhibited at the 18th Annual International Metallographic Society Meeting, Denver, CO, 21-24 July 1985. Received Third Place Award in Class 7b - Pretty Microstructures - Black and White Only. Part of a traveling international exhibit.

"Effect of Shot Peening Intensity and Recrystallization of Annealing on Surface Morphology of Ti-6Al-4V Castings," R. Brodecki, C. M. Cooke, J. T. Cammett, W. A. Houston, and D. Eylon, Exhibited at the International Metallographic Society 18th Annual Meeting, Denver, CO, 21-24 July 1985. Part of a traveling international exhibit.

"Fracture - Microstructure Correlations in Titanium Alloys," R. Brodecki, C. M. Cooke, W. A. Houston, and D. Eylon, Exhibited at the International Metallographic Society 18th Annual Meeting, Denver, CO, 21-24 July 1985. Part of a traveling international exhibit.



"'Tip' in Ti-6Al-4V Powder Compact," R. Brodecki, S. Schwenker, F. H. Froes, and D. Eylon, Exhibited at the International Metallographic Society 17th Annual Meeting, Philadelphia, PA, 15-18 July 1984. Received Honorable Mention and Ribbon on Class 6 - Electron Microscopy - Scanning. Part of a traveling international exhibit. Published in Metallography 18(1), 106 (February 1985).

"Nodular Graphite Surrounded by Ferrite in a Matrix of Perlite," C. E. Harper. Color photograph received honorable mention, Light Micrography, 1985 International Instant Photomicrography Competition sponsored by Polaroid.

"Illusion," R. Brodecki, S. Schwenker, D. Eylon, and F. H. Froes, Exhibited at the International Metallographic Society 17th Annual Meeting, Philadelphia, PA, 15-18 July 1984. Part of a traveling international exhibit.

"Big 'O'," S. D. Apt, Exhibited at the International Metallographic Society 17th Annual Meeting, Philadelphia, PA, 15-18 July 1984. Part of a traveling international exhibit.

"Alpha World," S. D. Apt and R. K. Lewis, Exhibited at the 17th Annual International Metallographic Society Conference and Metallographic Exhibit, Philadelphia, PA, 15-18 July 1984. Part of a traveling international exhibit.

"Large Grain Deformation in Ti-10V-2Fe-3Al," E. Harper with I. Weiss, Exhibited at the 17th Annual International Metallographic Society Conference and Metallographic Exhibit, Philadelphia, PA, 15-18 July 1984. Part of a traveling international exhibit.

"Sub-Boundaries in the Alpha Phase of Ti-64," E. Harper, I. Weiss, J. H. Steele, F. H. Froes, and D. Eylon, Exhibited at the 17th Annual International Metallographic Society Conference and Metallographic Exhibit, Philadelphia, PA, 15-18 July 1984. Part of a traveling international exhibit.

"Splash," E. Harper and S. D. Apt, Exhibited at the 17th Annual International Metallographic Society Conference and Metallographic Exhibit, Philadelphia, PA, 15-18 July 1984. Part of a traveling international exhibit.

"The Morphology of Cured Epoxy Resin," R. Omlor, P. F. Lloyd, L. T. Drzal, V. B. Gupta, and W. W. Adams, Exhibited at the 17th Annual International Metallographic Society Meeting, Philadelphia, PA, 15-18 July 1984. Received honorable mention and ribbon in Class 5 - Analytical Electron Microscopy. Part of a traveling international exhibit. Published in Metallography 18 (1), 106 (February 1985).

"Inclusion Analysis in Aluminum PM 7091 Alloy," R. E. Omlor, P. F. Lloyd and S. Kirchoff, Exhibited at the 17th Annual International Metallographic Society Meeting, Philadelphia, PA, 15-18 July 1984. Part of a traveling international Exhibit.

#### INVENTIONS

"Method of Making Powders by Electro-Discharge Machining in a Cryogenic Dielectric," E. Harper and S. J. Savage, Invention disclosed on October 12, 1984.

END

11-87

DTIC